JAERI-Tech
95-052

CORCON-MOD3 ANALYSIS OF SURC EXPERIMENTS ON MOLTEN CORE CONCRETE INTERACTION

December 1995

Jinquan YAN*, Yu MARUYAMA and Jun SUGIMOTO

日本原子力研究所
Japan Atomic Energy Research Institute

本レポートは，日本原子力研究所が不定期に公刊している研究報告書です。
入手の問合わせは，日本原子力研究所技術情報部情報資料課(〒319-11 茨城県那珂郡東海村）あて，お申し越しください。なお，このほかに財団法人原子力弘済会資料センター（〒319-11 茨城県那珂郡東海村日本原子力研究所内）で複写による実費頒布をおこなっております。

This report is issued irregularly.
Inquiries about availability of the reports should be addressed to Information Division, Department of Technical Information, Japan Atomic Energy Research Institute, Tokai-mura, Naka-gun, Ibaraki-ken 319-11, Japan.

編集兼発行　日本原子力研究所
印　　刷　㈱高野高速印刷

CORCON-Mod3 Analysis of SURC Experiments on Molten Core Concrete Interaction

Jinquan YAN*, Yu MARUYAMA and Jun SUGIMOTO

Department of Reactor Safety Research
Tokai Research Establishment
Japan Atomic Energy Research Institute
Tokai-mura, Naka-gun, Ibaraki-ken

(Received November 1, 1995)

The SURC series of molten core concrete interaction experiments carried out at Sandia National Laboratories was selected to be analyzed by CORCON-Mod3 code. Detailed comparisons between code calculations and experimental measurements were performed for thermal behaviors, gas releases and aerosol generations. It was found that thermal behaviors such as concrete erosion and melt temperature history were reasonably predicted by the code. Large discrepancies were shown in amount and composition of gas released. Especially, CORCON-Mod3 could not reproduce the continuous release of combustible gases (H_2 and CO) during the interactions. The discrepancies of gas releases might indicate that a kinetic approach is required on the reaction between metallic materials in the molten core and the concrete decomposed gases. Difference within one through several orders of magnitude were predicted for the releases of fission product simulants. In order to discuss more detail about adequacy of the models on the chemistry and vaporization of the molten core materials, the database of chemical species and related thermodynamic properties contained in CORCON-Mod3 should be extended.

Keywords : CORCON-Mod3, SURC Experiments, Molten Core Concrete Interaction Thermal History, Gas Release, Aerosol Generation, Fission Product

---

The present work was performed while one of authors (Jinquan Yan) stayed at JAERI, Tokai Research Establishment, from September 1994 to March 1995 under Scientist Exchange Program by Science and Technology Agency of Japan.

* Shanghai Nuclear Engineering Research and Design Institute

ＣＯＲＣＯＮ－Ｍｏｄ３による溶融炉心コンクリート相互作用に関するＳＵＲＣ実験の解析

日本原子力研究所東海研究所原子炉安全工学部
Jinquan YAN＊・丸山　結・杉本　純

（1995年11月１日受理）

ＣＯＲＣＯＮ－Ｍｏｄ３コードを用いて，サンディア国立研究所で行われた溶融炉心コンクリート相互作用に関するＳＵＲＣ実験の解析を実施した。熱的挙動，気体の発生及びエアロゾルの生成について実験結果と解析結果の詳細な比較を行った。ＣＯＲＣＯＮ－Ｍｏｄ３はコンクリートの溶融浸食，溶融物の温度履歴等の熱的挙動を比較的良く予測した。気体の発生量及び発生気体の組成については，解析と実験との差が大きいことが判明した。特に，ＣＯＲＣＯＮ－Ｍｏｄ３は，相互作用中における可燃性気体（H_2及びＣＯ）の連続的な発生を再現することができなかった。気体発生に関する解析と実験との差異は，溶融炉新内の金属質物質とコンクリート分解気体との化学反応に対する速度論的アプローチの必要性を示唆しているもの考えられる。ＦＰ模擬物の比較では，実験と解析結果に一桁から数桁の違いがあった。溶融物内の化学反応及び蒸発に関するモデルの妥当性をより詳細に検討するためには，コード内に含まれている化学種及び関連する熱力学的性質に関するデータベースを拡張することが必要であると考えられる。

本研究は，著者の一人（Jinquan Yan）が1994年９月から1995年３月にかけて，科学技術庁原子力研究交流制度に基づいて原研東海研究所に滞在している間に実施されたものである。
那珂研究所：〒319－11　茨城県那珂郡東海村白方白根2-4
＊　上海核工程研究設計院

Contents

目　　次

1. Introduction

Molten Core Concrete Interaction (MCCI) occur when a reactor vessel is molten-through and molten core materials drop onto the reactor cavity basemat during the late phase of a postulated severe accident in a light water reactor nuclear power plant. In the process of MCCI, a large amount of H_2O and CO_2 will be generated due to decomposition of concrete. A significant amount of H_2 and CO can be also produced by chemical reactions between the decomposed gases and the molten core materials. If the molten core is covered by an overlying water layer during MCCI, the water will be vaporized through a coolant boiling process. Accumulation of these vapors and noncondensable gases and/or burning of combustible gases will lead to the pressurization of a containment vessel, and continuous melt concrete interactions will erode the containment basemat, either may threaten the containment integrity. A large amount of radioactive fission products (FPs) may be released to the environment, should containment failure occurs.

Up to date MCCI is still an unwell-known area and is one of major contributors to the uncertainties of severe accident risks[1]. Since the progression of MCCI may significantly affect severe accident scenarios as well as offsite consequences, great efforts have been paid to the study on phenomena related to MCCI. In recent years, various MCCI experiments, especially those large scale experiments such as SURC series[2,3,4,5], BETA series[6] and ACE project L series[7], have been carried out. An experimental series on MCCI is included in ALPHA (Assessment of Loads and Performance of Containment in a Hypothetical Accident) program at JAERI (Japan Atomic Energy Research Institute)[8]. On the other hand, various computer codes, such as CORCON[9,10], WECHSL[11] and DECOMP[12], have been developed to model complicated processes during MCCI. The results from those MCCI experiments provide a wide range database for benchmarking of these computer codes. The validation efforts of these MCCI codes are now on going. In the previous research at JAERI[8,13], the ACE project L series experiments and the MCCI scoping experiment of the ALPHA program have been selected and analyzed by CORCON-Mod2[9] or CORCON-Mod3[10]. In the present study, the SURC MCCI experiments were selected to be analyzed by CORCON-Mod3, the latest version of CORCON code. The purposes of the present study are to make a better understanding of the MCCI process, and to validate CORCON-Mod3 code through the comparison between the SURC experiments and calculations.

2. Outline of SURC Experiments

The SURC MCCI experiments were designed and conducted at Sandia National Laboratories. Major characteristics of the SURC experiments are summarized in Table 1. The purposes of the SURC series MCCI experiments were to study; (1) heat transfer and concrete basemat ablation, (2) chemical reaction and combustible gas production, and (3) FP aerosol generation and release during MCCI processes. Both separated effect experiments using stainless steel (SURC-3 and SURC-4) as well as integral experiments using prototypical materials consisting mainly of UO_2 and ZrO_2 (SURC-1 and SURC-2) were conducted. In the present study, the

1. Introduction

Molten Core Concrete Interaction (MCCI) occur when a reactor vessel is molten-through and molten core materials drop onto the reactor cavity basemat during the late phase of a postulated severe accident in a light water reactor nuclear power plant. In the process of MCCI, a large amount of H_2O and CO_2 will be generated due to decomposition of concrete. A significant amount of H_2 and CO can be also produced by chemical reactions between the decomposed gases and the molten core materials. If the molten core is covered by an overlying water layer during MCCI, the water will be vaporized through a coolant boiling process. Accumulation of these vapors and noncondensable gases and/or burning of combustible gases will lead to the pressurization of a containment vessel, and continuous melt concrete interactions will erode the containment basemat, either may threaten the containment integrity. A large amount of radioactive fission products (FPs) may be released to the environment, should containment failure occurs.

Up to date MCCI is still an unwell-known area and is one of major contributors to the uncertainties of severe accident risks[1]. Since the progression of MCCI may significantly affect severe accident scenarios as well as offsite consequences, great efforts have been paid to the study on phenomena related to MCCI. In recent years, various MCCI experiments, especially those large scale experiments such as SURC series[2,3,4,5], BETA series[6] and ACE project L series[7], have been carried out. An experimental series on MCCI is included in ALPHA (Assessment of Loads and Performance of Containment in a Hypothetical Accident) program at JAERI (Japan Atomic Energy Research Institute)[8]. On the other hand, various computer codes, such as CORCON[9,10], WECHSL[11] and DECOMP[12], have been developed to model complicated processes during MCCI. The results from those MCCI experiments provide a wide range database for benchmarking of these computer codes. The validation efforts of these MCCI codes are now on going. In the previous research at JAERI[8,13], the ACE project L series experiments and the MCCI scoping experiment of the ALPHA program have been selected and analyzed by CORCON-Mod2[9] or CORCON-Mod3[10]. In the present study, the SURC MCCI experiments were selected to be analyzed by CORCON-Mod3, the latest version of CORCON code. The purposes of the present study are to make a better understanding of the MCCI process, and to validate CORCON-Mod3 code through the comparison between the SURC experiments and calculations.

2. Outline of SURC Experiments

The SURC MCCI experiments were designed and conducted at Sandia National Laboratories. Major characteristics of the SURC experiments are summarized in Table 1. The purposes of the SURC series MCCI experiments were to study; (1) heat transfer and concrete basemat ablation, (2) chemical reaction and combustible gas production, and (3) FP aerosol generation and release during MCCI processes. Both separated effect experiments using stainless steel (SURC-3 and SURC-4) as well as integral experiments using prototypical materials consisting mainly of UO_2 and ZrO_2 (SURC-1 and SURC-2) were conducted. In the present study, the

SURC-4, SURC-1 and SURC-2 experiments were selected to be modeled and analyzed with CORCON-Mod3 code since these were relatively large scale experiments with fairly reliable instrumentation.

2.1 SURC-4

The SURC-4 was a separated effect experiment. It was designed to investigate the additional effect of zirconium (Zr) metal on steel melt interactions with basaltic concrete. This type of concrete has a high SiO_2 content (56 w/o) and typically releases 5 w/o H_2O and 1.5 w/o CO_2 when it is heated to ablation.

The SURC experimental geometry is shown in Fig. 1. The interaction crucible used in the SURC-4 experiment had a 0.4 m thick basaltic concrete basemat which was surrounded by an MgO annulus sidewall having an inner diameter of 0.4 m. The interaction crucible was such designed to limit concrete erosion to a downward or an axial direction. The crucible was enclosed with a water-cooled aluminum (Al) containment vessel that was purged with argon gas during the experiment. Gases and aerosols produced during melt concrete interactions were collected and sampled through a flow tube flanged to the top of the containment vessel. The experiment was instrumented to measure various parameters, such as concrete ablation, melt temperature, gas generation, gas composition, and aerosol characteristics.

The charge materials used in the SURC-4 consisted of 200 kg stainless steel as well as 6 kg FP simulants. During the experiment, the charge materials in the interaction crucible were inductively heated. After about 105 minutes heating, the steel charge began to melt and that resulted in rapid ablation of the basemat concrete. After a constant concrete ablation rate was observed, 20 kg of metallic Zr was added into the melt pool to study the effect caused by Zr addition. As a result, the concrete ablation rate as well as gas generation rate were drastically increased. A total depth of 0.24 to 0.27 m basaltic concrete were eroded during over 60 minutes melt concrete interactions.

2.2 SURC-1 and SURC-2

The SURC-1 and SURC-2 were large-scale integral experiments on interactions of molten UO_2-ZrO_2-Zr mixture with limestone (SURC-1) or basaltic (SURC-2) concrete. The experiments were conducted in a very similar thermal history so as to show the differences in behaviors of limestone and basaltic concrete during interactions with the high temperature melt.

In the SURC-1 and SURC-2 experiments, the same geometry and instrumentation scheme as in the SURC-4 were used. The charge materials both in the SURC-1 and SURC-2 consisted of 200 kg mixture of UO_2 (69 w/o), ZrO_2 (23 w/o) and Zr (8 w/o) along with 3.364 kg of FP simulants. Because the oxidic charge did not couple efficiently to the induction power supply, five tungsten (W) rings were embedded within the charge. The tungsten rings were heated by the induction power supply and then transferred heat to the oxidic charge during the experiments.

After 130 minutes of heating, concrete ablation was detected. In the early stage, the ablation

rate was quite rapid as Zr in the charge was oxidized. After termination of the Zr oxidation, the ablation rate decreased significantly. At about 40 minutes after the onset of the concrete ablation, the power supply was increased, and again a more vigorous interaction was observed both in the SURC-1 and in the SURC-2. A total concrete depth of 0.24 to 0.27 m in the SURC-1 and 0.30 to 0.35 m in the SURC-2 was eroded during over 130 minutes melt concrete interactions.

3. Analytical Methods

The latest version of CORCON code, CORCON-Mod3, was used to perform post-test analyses of the SURC experiments. In CORCON-Mod3, several new models were added and some improvements were made over the previous version. Some of these new models and improvements are listed below;

(1) slag film melt-concrete heat transfer model,
(2) coolant film boiling heat transfer model,
(3) bubble behavior model,
(4) inclusion of VANESA[14] model as a subroutine,
(5) condensed phase chemistry model, and
(6) aerosol scrubbing model for subcooled overlying water pools.

3.1 Modeling of SURC-4

In the calculation, all the charge materials were considered to participate in the interaction and the melt composition were directly taken from the experimental documentation[2]. The basaltic concrete composition was also from the documentation. As mentioned above, the melt concrete interaction in the SURC-4 was one dimensional (limited to a downward direction). Since CORCON-Mod3 usually deals with two dimensional erosion, the time dependent debris radius model was activated to restrict the interactions only in the downward direction. A constant debris radius (crucible radius, 0.2 m) was used, and thus the radial heat flux was set to be zero. To keep energy balance, the sidewall heat loss in the experiment was subtracted from the net induction input power to the melt pool. The net induction power history was prepared based on the experimental documentation. The sidewall heat loss in the experiment was estimated by means of multiplying the measured sidewall heat flux to the melt pool perimetric area contacted to the crucible sidewall. Heat loss from the top of the melt pool was modeled by adjusting emissivity of surroundings so as to match the measured value.

The CORCON calculation started with the onset of melt concrete interaction. The temperature of melt at the onset of the concrete ablation was assumed to be 1780 K according to the experimental documentation. The addition of 20 kg Zr to the melt started at 119 minutes into the experiment and completed within 90 seconds. A two layers melt pool configuration (metallic and oxidic layers) was assumed with an inter-layer mixing model disabled during the melt concrete interactions. The new melt-concrete heat transfer model (slag film model) was used. The condensed phase chemistry model was activated since SiO_2 rich basaltic concrete was used in the SURC-4 experiment. The VANESA calculation for aerosol releases

rate was quite rapid as Zr in the charge was oxidized. After termination of the Zr oxidation, the ablation rate decreased significantly. At about 40 minutes after the onset of the concrete ablation, the power supply was increased, and again a more vigorous interaction was observed both in the SURC-1 and in the SURC-2. A total concrete depth of 0.24 to 0.27 m in the SURC-1 and 0.30 to 0.35 m in the SURC-2 was eroded during over 130 minutes melt concrete interactions.

3. Analytical Methods

The latest version of CORCON code, CORCON-Mod3, was used to perform post-test analyses of the SURC experiments. In CORCON-Mod3, several new models were added and some improvements were made over the previous version. Some of these new models and improvements are listed below;

(1) slag film melt-concrete heat transfer model,
(2) coolant film boiling heat transfer model,
(3) bubble behavior model,
(4) inclusion of VANESA[14] model as a subroutine,
(5) condensed phase chemistry model, and
(6) aerosol scrubbing model for subcooled overlying water pools.

3.1 Modeling of SURC-4

In the calculation, all the charge materials were considered to participate in the interaction and the melt composition were directly taken from the experimental documentation[2]. The basaltic concrete composition was also from the documentation. As mentioned above, the melt concrete interaction in the SURC-4 was one dimensional (limited to a downward direction). Since CORCON-Mod3 usually deals with two dimensional erosion, the time dependent debris radius model was activated to restrict the interactions only in the downward direction. A constant debris radius (crucible radius, 0.2 m) was used, and thus the radial heat flux was set to be zero. To keep energy balance, the sidewall heat loss in the experiment was subtracted from the net induction input power to the melt pool. The net induction power history was prepared based on the experimental documentation. The sidewall heat loss in the experiment was estimated by means of multiplying the measured sidewall heat flux to the melt pool perimetric area contacted to the crucible sidewall. Heat loss from the top of the melt pool was modeled by adjusting emissivity of surroundings so as to match the measured value.

The CORCON calculation started with the onset of melt concrete interaction. The temperature of melt at the onset of the concrete ablation was assumed to be 1780 K according to the experimental documentation. The addition of 20 kg Zr to the melt started at 119 minutes into the experiment and completed within 90 seconds. A two layers melt pool configuration (metallic and oxidic layers) was assumed with an inter-layer mixing model disabled during the melt concrete interactions. The new melt-concrete heat transfer model (slag film model) was used. The condensed phase chemistry model was activated since SiO_2 rich basaltic concrete was used in the SURC-4 experiment. The VANESA calculation for aerosol releases

during the interaction was also included.

3.2 Modeling of SURC-1 and SURC-2

The modeling methods for the SURC-1 and SURC-2 were quite similar. The post-test examinations showed that a portion of the charge materials was either not molten or remained in the upper region between the top two of the five tungsten rings. These charge materials were assumed not to participate in the interactions with the basemat concrete during the experiments. In another words, only 60% of the 200 kg charge with the same composition as in the experiments were considered in the calculations for the SURC-1 and SURC-2 experiments. The melt pool temperature at the onset of the concrete ablation was assumed to be 2600 K in the SURC-1 and 2650 K in the SURC-2 experiment.

As in modeling of the SURC-4 experiment, the melt pool radius was also set to the radius of the MgO crucible for the SURC-1 and SURC-2 by means of activation of the time dependent pool radius model to simulate the axial one dimensional melt concrete interaction. The radial heat transfer was thus set to be zero. The sidewall heat losses in the experiments were subtracted from the net induction power. The net induction power given in the experimental documentation[3,4] was multiplied by a factor of 0.6 in consistent with the consideration of the melt mass. The sidewall heat loss was estimated using the same method as in the SURC-4 simulation. Since there were charge materials remained between the top tungsten rings which were inductively heated during the experiment, heat loss from the melt pool top was not considered in the analyses of the SURC-1 and SURC-2. A one layer melt pool configuration was assumed. The melt was assumed to be well mixed and remained mixing during the melt concrete interaction. The slag film melt-concrete heat transfer model was used both in the SURC-1 and SURC-2 simulations. The condensed phase chemistry model was disabled in the SURC-1 simulation because SiO_2 poor limestone concrete was used, but enabled in the SURC-2 calculation since the condensed phase chemistry was realized to be important in melt interaction with SiO_2 rich basaltic concrete.

4. Results of Analysis

4.1 SURC-4

Comparisons between the calculations and the measurements for concrete ablation depth and melt pool temperature of the SURC-4 are given in Figs. 2a and 3a, respectively. Figure 2a shows a relatively good agreement for the concrete ablation depth between the calculation and the measurement. The melt temperature history shown in Fig. 3a indicates that the peak melt temperature resulted from the violent Zr oxidation was underpredicted by 80 K. In CORCON-Mod3, it is assumed that the metallic material is added to the metallic layer where condensed SiO_2 is not rich in the two layers melt pool configuration modeling. It can be expected that the calculated melt temperature rise caused by the Zr oxidation may be higher if Zr is added to the SiO_2 rich region. This was confirmed by another sensitivity calculation. In this calculation, it was assumed that the melt pool materials were well mixed to form

during the interaction was also included.

3.2 Modeling of SURC-1 and SURC-2

The modeling methods for the SURC-1 and SURC-2 were quite similar. The post-test examinations showed that a portion of the charge materials was either not molten or remained in the upper region between the top two of the five tungsten rings. These charge materials were assumed not to participate in the interactions with the basemat concrete during the experiments. In another words, only 60% of the 200 kg charge with the same composition as in the experiments were considered in the calculations for the SURC-1 and SURC-2 experiments. The melt pool temperature at the onset of the concrete ablation was assumed to be 2600 K in the SURC-1 and 2650 K in the SURC-2 experiment.

As in modeling of the SURC-4 experiment, the melt pool radius was also set to the radius of the MgO crucible for the SURC-1 and SURC-2 by means of activation of the time dependent pool radius model to simulate the axial one dimensional melt concrete interaction. The radial heat transfer was thus set to be zero. The sidewall heat losses in the experiments were subtracted from the net induction power. The net induction power given in the experimental documentation[3,4] was multiplied by a factor of 0.6 in consistent with the consideration of the melt mass. The sidewall heat loss was estimated using the same method as in the SURC-4 simulation. Since there were charge materials remained between the top tungsten rings which were inductively heated during the experiment, heat loss from the melt pool top was not considered in the analyses of the SURC-1 and SURC-2. A one layer melt pool configuration was assumed. The melt was assumed to be well mixed and remained mixing during the melt concrete interaction. The slag film melt-concrete heat transfer model was used both in the SURC-1 and SURC-2 simulations. The condensed phase chemistry model was disabled in the SURC-1 simulation because SiO_2 poor limestone concrete was used, but enabled in the SURC-2 calculation since the condensed phase chemistry was realized to be important in melt interaction with SiO_2 rich basaltic concrete.

4. Results of Analysis

4.1 SURC-4

Comparisons between the calculations and the measurements for concrete ablation depth and melt pool temperature of the SURC-4 are given in Figs. 2a and 3a, respectively. Figure 2a shows a relatively good agreement for the concrete ablation depth between the calculation and the measurement. The melt temperature history shown in Fig. 3a indicates that the peak melt temperature resulted from the violent Zr oxidation was underpredicted by 80 K. In CORCON-Mod3, it is assumed that the metallic material is added to the metallic layer where condensed SiO_2 is not rich in the two layers melt pool configuration modeling. It can be expected that the calculated melt temperature rise caused by the Zr oxidation may be higher if Zr is added to the SiO_2 rich region. This was confirmed by another sensitivity calculation. In this calculation, it was assumed that the melt pool materials were well mixed to form

single layer. The results are given in Figs. 2b and 3b. Figure 3b shows a good agreement between the calculated and measured melt temperature. However, the prediction of the ablation depth shown in Fig. 2b was not as good as the first calculation. The calculated ablation rate seemed to be lower than the measurements during the initial period when there was no Zr in the melt pool and during later phase when the added Zr was fully oxidized. On the other hand, the calculated ablation rate was higher in the middle period during the Zr oxidation, though the maximum concrete erosion depth was reasonably compared with the experimental result. The lower ablation rate was due to the lower heat transfer, which might be attributed to the lower (compared with the metallic layer in the first calculation) averaged thermal conductivity of the mixed melt adjacent to the concrete basemat. Energy balance and metal mass for the above two calculations are given in Figs. 4a, 4b and 5a, 5b, respectively. In consistence with the higher peak of melt temperature in the sensitivity calculation, Zr oxidation rate (Fig. 5b) and heat generation rate (Fig. 4b) were more rapid under the single layer assumption than those (Figs. 5a and 4a) under the two layers assumption. These comparisons for the thermal behaviors of the melt concrete interaction should suggest that the inter-layer mixing between metallic and oxidic layers and accompanied changes of material properties are of great importance to adequately simulate MCCI thermal processes.

The calculated composition and amount of gases released are given in Figs. 6 and 7, respectively. In the calculation, almost all of the concrete decomposed CO_2 and H_2O were reduced to CO and H_2 due to metal-gas chemical reactions, while in the experiment, the released gas composition during the initial period when there was no Zr in the melt (100-120 minutes) was 65% H_2, 20% CO, 5% H_2O and 10% CO_2, and after Zr addition the gas composition was 83% H_2, 14% CO, 1% H_2O and 1% CO_2. The differences of the gas composition between the calculation and the measurement before the Zr addition may be attributed to a chemical equilibrium assumption of the code. In CORCON-Mod3, it is assumed that a chemical equilibrium state is achieved between the reactants during a short time interval. This may not be true when the melt pool is not so thick and the time for gas bubbles to pass through the melt is not so long in the experimental conditions. Figure 7 shows that the calculated total gas generation was 212 moles corresponding to a total erosion depth of 0.23 m basaltic concrete. In the experiment, the collected gases were 241 moles, and a total erosion depth of 0.24 to 0.27 m was measured. The calculated amount of released gases agreed reasonably well with the experimental result.

In the SURC-4 experiment, the post-test examination showed that the aerosol sampling pipe was narrowed or even plugged during some time periods by the foamy materials generated probably from the Zr oxidation. Also the aerosol data after Zr addition showed a large discrepancy by different samplers. Thus aerosol data comparison was attempted only for the initial time period before the Zr addition. The aerosol concentration collected during this period ranged from 6 g/m^3 to 17 g/m^3 at the standard temperature and pressure. The calculated aerosol concentration is shown in Fig. 8, which indicates that CORCON-Mod3 overpredicted the aerosol concentration by a factor of 10. It should be noted that CORCON-Mod3 calculates the aerosol concentration just above the melt surface. Therefore, since the aerosol concentration decreases due to aerosol deposition over the path from the interaction crucible to the aerosol sampling system, the difference between the experiment and the calculation should have been smaller if the comparison was made at an identical location.

During this period, the experiment showed that the filtered aerosols were dominated by the concrete materials and tellurium (Te) as a FP simulant with an averaged composition of 67.9% Te, 4.2% potassium (K), 3.0% sodium (Na), 1.5% silicon (Si), 3.2% manganese (Mn) and 1.2% chromium (Cr). Fission product simulants, molybdenum (Mo) and cerium (Ce), were also found (approximately 0.03% and 0.08% respectively), while barium (Ba) and lanthanum (La) were under a detectable limit (0.02%). The CORCON-Mod3 calculation showed that the aerosol was also dominated by the concrete materials and Te but a quite different composition as 4% Te, 55% K, 35% Na and 5% Si (Fig. 9), accompanied by a small amount of other FP simulants (Fig. 10). The CORCON-Mod3 calculation overpredicted release of Ba, but underpredicted releases of Te and Ce by up to one order and Mo by several orders of magnitude.

The chemistry of the molten materials during MCCIs may include considerably complex processes due to the formation of a multi-component mixture with the elevated temperature. These complex processes make it difficult to model the chemical processes of MCCIs. A chemical equilibrium approach is used in many computer codes. The same approach is adopted in VANESA with a consideration of the surface area limitation available for a mass transfer. The chemical equilibrium approach requires appropriate chemistry data which include chemical species and related thermodynamic properties (Gibbs free energy of formation). The difference between the experiment and the prediction must be partly resulted from insufficient coverage of the chemistry data in VANESA module of CORCON-Mod3. Further discussions will be made for assessment of the VANESA approach of the chemistry modeling by adequately extending the chemical species and thermodynamic properties data. The molten materials are assumed in VANESA to form two layers, an oxidic layer rested on a metallic layer. The chemical equilibrium calculations are made for each layers separately. Therefore, the direct chemical reactions between the metallic and the oxidic materials can not be treated by VANESA. This assumption in VANESA on the melt configuration is considered to be another possible reason to cause the difference.

4.2 SURC-1

Comparisons between the measurements and the calculations for concrete ablation depth and melt temperature of the SURC-1 is shown in Figs. 11 and 12, respectively. It can be seen that, the concrete ablation depth was well predicted though the ablation rate during the initial stage when Zr existed in the melt seemed to be slightly underpredicted by the code. The calculated melt temperature underestimated the measurement during the initial and the middle stages, and overpredicted by 100 K to 200 K in the later stage after the input power was increased in the experiment.

Figures 13 and 14 show the calculated composition and amount of released gas for the SURC-1. According to the calculation, almost all of the decomposed CO_2 and H_2O were reduced to CO and H_2 due to Zr-gas reactions. Again this might be attributed to the chemical equilibrium assumption in the chemical reaction model of the code, as was explained in the analysis of the SURC-4 experiment. After termination of the Zr oxidation, CO_2 and H_2O were released instead of CO and H_2. The experiment showed a gas composition of 5% H_2,

5% H_2O, 84% CO and 6% CO_2 during the initial stage with existence of Zr in the melt, a composition of 7% H_2, 8% H_2O, 75% CO and 10% CO_2 in the middle stage when the Zr oxidation completed and the input power was still low, and a composition of 5% H_2, 5% H_2O, 75% CO and 10% CO_2 in the later stage when input power was increased. The measurement showed that CO and H_2 were continuously released and CO was always the dominant species (no less than 75% in volume) of the released gas mixture. However this was not predicted well in the calculation. In the SURC-1 experiment, the total amount of collected gas mixture (excluding argon gas) was 379 moles, while in the calculation the total amount of gas mixture was 720 moles. There was large discrepancy between the experimental measurements and the calculated results for both the gas composition and the total amount of gas released.

It should be noted that the condensed phase chemistry model was not used in the above calculation, because the metal-gas reaction might be much more important than the condensed phase chemistry when the interacting concrete contains a large amount of gas species which was the situation of the SURC-1 experiment. Nevertheless, a comparison calculation was performed with the condensed phase chemistry model. However, as was expected, little change was found since the current condensed phase chemistry model takes Zr-SiO_2 reaction as a major reaction and there was only 3.6% of SiO_2 in the limestone concrete of the SURC-1 experiment. Figure 15 shows the calculated metal mass with the condensed phase chemistry model. The slight formation of metallic Si and Al was predicted due to chemical reactions of SiO_2 and Al_2O_3 with Zr in the initial stage.

A simple calculation was also performed to check if the code calculated a correct result for the total amount of decomposed gases. The content of CO_2 and H_2O in the limestone concrete used in the SURC-1 was 35.7 w/o and 4.1 w/o, respectively. Considering 0.23 m thick (calculated total erosion depth for the SURC-1 experiment) limestone concrete slug with a diameter of 0.4 m and a density of 2400 kg/m^3, the total concrete mass, the decomposed CO_2 mass and H_2O mass are calculated as follows.

$$M_{CON} = \pi D^2 H \rho / 4$$
$$= 3.14 \times 0.42 \times 0.23 \times 2400/4$$
$$= 69.33 \text{ kg}$$

$$M_{CO2} = 35.7\% M_{CON}$$
$$= 24.75 \text{ kg}$$
$$= 562.5 \text{ mole}$$

$$M_{H2O} = 4.1\% M_{CON}$$
$$= 2.84 \text{ kg}$$
$$= 157.7 \text{ mole}$$

Where, M_{CON}, M_{CO2} and M_{H2O} denote the mass of concrete, CO_2 and H_2O, respectively. That means, if 0.23 m limestone concrete ablated in the SURC-1 experiment, the total amount of decomposed gas mixture of CO_2 and H_2O should have been 720 moles. Some of these decomposed gases were reduced to CO and H_2 due to chemical reactions with metallic Zr or other species. But the total amount of mixture of decomposed gases (CO_2 and H_2O) and the

reaction products (CO and H_2) should have also been 720 moles if no or little other species such as elemental carbon (C) were generated during the chemical reactions.

The gas mixture of 379 moles consisting primarily of CO, CO_2, H_2 and H_2O was collected during the SURC-1 experiment. This amount was approximately a half of the initial contents of CO_2 and H_2O in the ablated concrete basemat which could be released during the interaction. The composition of CO, CO_2, H_2 and H_2O in the collected gas mixture was 75-84%, 6-10%, 5-7% and 5-8%, respectively. Taking an average value of the gas composition, 301 moles of CO and 23 moles of H_2 were produced by chemical reactions in the melt layer. Metallic Zr must have been a dominant material to reduce CO_2 and H_2O to CO and H_2, respectively. The amount of CO and H_2 in the collected gas mixture is considered to be consistent with the mass of Zr in the melt (182 moles) since one mole of Zr could generate two moles of CO or H_2.

Regarding the difference between the initially contained amount of CO_2 and H_2O (720 moles) and the amount of the collected gas mixture (379 moles), detailed discussions were not possible due to insufficient information in the experimental documentation[3]. A coking reaction of CO_2 with metallic materials to produce C is supposed to be a possible reason for the disappearance of CO_2. According to an oxidation-reduction equilibrium diagram, Zr and reduced products of the concrete decomposed materials (i. e. reduction of SiO_2, MgO, and Al_2O_3 to Si, magnesium (Mg) and Al) would be candidates to contribute to the coking reaction. Tungsten, which was used as a susceptor rings in the experiment, could be eliminated from the candidates since CO is much more stable than tungsten oxide at the elevated temperature. It is currently uncertain, however, whether the coking reaction progresses significantly during the interaction of the molten core with a CO_2 rich concrete basemat. Further study will be required to well understand the chemical behavior in the molten core materials.

4.3 SURC-2

Comparisons between the calculations and the experiments for concrete erosion depth and melt temperature of the SURC-2 experiment are shown in Figs. 16 and 17, respectively. The comparisons showed good agreements for both erosion depth and melt temperature history. The rise of the measured melt temperature in the later stage shown in Fig. 17 was an expected behavior resulted from the increase of the input power, and that was reproduced by the code calculation.

The calculated composition and total amount of released gases are shown in Figs. 18 and 19, respectively. The calculated total amount of released gases was 340 moles, while the collected amount of released gases in the SURC-2 experiment was 272 moles. As in the analysis of the SURC-1 experiment, almost all of the decomposed CO_2 and H_2O were reduced to CO and H_2 when metallic Zr and/or condensed phase reaction products such as Si existed in the melt (Fig. 20). After Zr and Si were fully oxidized, CO_2 and H_2O were released instead of CO and H_2. In the SURC-2 experiment, the released gas had a composition of 75% H_2, 5% H_2O, 15% CO and 5% CO_2 in the initial stage when Zr existed in the melt, a composition of 70% H_2, 5% H_2O, 15% CO and 10% CO_2 in the middle stage when Zr was oxidized and the input

power was still low, and a composition of 75% H_2, 5% H_2O, 15% CO and 10% CO_2 in the later stage when input power was increased. During the interaction, H_2 and CO were continuously released and H_2 was the dominated species (no less than 70% in volume) among the released gas mixture. Again this was not well predicted by the code, though the calculated results were improved compared with the analysis of the SURC-1 experiment.

The VANESA calculation was included in the analysis of the SURC-2 experiment though it was believed that the difference in released gas composition and amount between the calculation and the experiment would have corresponding influences on aerosol releases. The calculated aerosol concentration for the SURC-2 is shown in Fig. 21. Before fully oxidation of Si, the aerosol concentration was approximately 1.2 kg/m^3 and after that it dropped to 0.2 kg/m^3. In the experiment, the aerosol concentration ranged from 15 to 300 g/m^3, with an averaged concentration of 90 g/m^3 in the early stage, 50 g/m^3 in the middle stage and 40 g/m^3 in the later stage. The VANESA calculation overpredicted the aerosol concentration by a factor of 5 to 13.

In the experiment, the released aerosol was dominated by concrete materials as shown in Fig. 22, typically 5-30% Na, 1-20% K, 10-25% Si, with a little amount of Mg (0.01-2%, either from the crucible or from the concrete), uranium (U) (0.1-0.3%, from the melt pool) and W (0.05-30%, from the tungsten assembly). The FP simulants Mo (0.005-0.4%) and Ba (0.002-0.06%) were also present, which is shown in Fig. 23, but little or no trace of La and Ce were found and Nb was under a detectable limit (0.001%). The calculation also showed that the dominant aerosol materials were concrete decomposed products, Na (5-15%), K (10-40%) and Si (0-80%) (Fig. 24), with a small amount of FP simulants (Fig. 25) before fully oxidation of Si (170 minutes). Differences within one to several orders of magnitude were found between the experiment and the calculation. Especially for the release of Mo, the difference reached 6 orders of magnitude, and a qualitative tendency in the experiment, that the release of Mo increased with time, could not be predicted by VANESA module of CORCON-Mod3. Figures 24 and 25 show that after accomplishment of Si oxidation, the aerosol composition changed drastically. This was attributed to a sudden change of the chemical conditions (oxygen potential) of the melt pool.

5. Summary and Conclusions

CORCON-Mod3 code was used to perform post-test analyses for the SURC-1, SURC-2 and SURC-4 MCCI experiments. The comparisons between the calculated results and the experimental measurements showed that when the slag film melt-concrete heat transfer model was used, the CORCON-Mod3 code was able to give reasonable predictions for thermal behaviors, such as concrete ablation and melt pool temperature history especially for melt interactions with basaltic concrete. It was found that the configuration of the molten material layers (single or multi-layer) strongly influenced the thermal behaviors of MCCIs when the melt contained a large amount of metallic materials. This suggests that the inter-layer mixing and its influence on properties of molten materials are of great importance for the prediction of MCCI.

power was still low, and a composition of 75% H_2, 5% H_2O, 15% CO and 10% CO_2 in the later stage when input power was increased. During the interaction, H_2 and CO were continuously released and H_2 was the dominated species (no less than 70% in volume) among the released gas mixture. Again this was not well predicted by the code, though the calculated results were improved compared with the analysis of the SURC-1 experiment.

The VANESA calculation was included in the analysis of the SURC-2 experiment though it was believed that the difference in released gas composition and amount between the calculation and the experiment would have corresponding influences on aerosol releases. The calculated aerosol concentration for the SURC-2 is shown in Fig. 21. Before fully oxidation of Si, the aerosol concentration was approximately 1.2 kg/m^3 and after that it dropped to 0.2 kg/m^3. In the experiment, the aerosol concentration ranged from 15 to 300 g/m^3, with an averaged concentration of 90 g/m^3 in the early stage, 50 g/m^3 in the middle stage and 40 g/m^3 in the later stage. The VANESA calculation overpredicted the aerosol concentration by a factor of 5 to 13.

In the experiment, the released aerosol was dominated by concrete materials as shown in Fig. 22, typically 5-30% Na, 1-20% K, 10-25% Si, with a little amount of Mg (0.01-2%, either from the crucible or from the concrete), uranium (U) (0.1-0.3%, from the melt pool) and W (0.05-30%, from the tungsten assembly). The FP simulants Mo (0.005-0.4%) and Ba (0.002-0.06%) were also present, which is shown in Fig. 23, but little or no trace of La and Ce were found and Nb was under a detectable limit (0.001%). The calculation also showed that the dominant aerosol materials were concrete decomposed products, Na (5-15%), K (10-40%) and Si (0-80%) (Fig. 24), with a small amount of FP simulants (Fig. 25) before fully oxidation of Si (170 minutes). Differences within one to several orders of magnitude were found between the experiment and the calculation. Especially for the release of Mo, the difference reached 6 orders of magnitude, and a qualitative tendency in the experiment, that the release of Mo increased with time, could not be predicted by VANESA module of CORCON-Mod3. Figures 24 and 25 show that after accomplishment of Si oxidation, the aerosol composition changed drastically. This was attributed to a sudden change of the chemical conditions (oxygen potential) of the melt pool.

5. Summary and Conclusions

CORCON-Mod3 code was used to perform post-test analyses for the SURC-1, SURC-2 and SURC-4 MCCI experiments. The comparisons between the calculated results and the experimental measurements showed that when the slag film melt-concrete heat transfer model was used, the CORCON-Mod3 code was able to give reasonable predictions for thermal behaviors, such as concrete ablation and melt pool temperature history especially for melt interactions with basaltic concrete. It was found that the configuration of the molten material layers (single or multi-layer) strongly influenced the thermal behaviors of MCCIs when the melt contained a large amount of metallic materials. This suggests that the inter-layer mixing and its influence on properties of molten materials are of great importance for the prediction of MCCI.

Large discrepancies were found between the calculations and the measurements for composition and amount of released gases. In the analysis of the experiment on the oxidic melt interaction with limestone concrete, CORCON-Mod3 largely overpredicted the total amount of released gas by a factor of up to 2 along with a quite different gas composition. Regarding the MCCI experiments with basaltic concrete, the calculations for the total amount of gas generated showed reasonable agreement with the experimental observation. However, the continuous release of reduced products (H_2 and CO) of concrete decomposed gases could not be reproduced by CORCON-Mod3. The difference between the experimental results and calculations might indicate that a kinetic approach is required for the chemical reactions between metallic materials and concrete decomposed gases.

The VANESA calculations were performed for the SURC-4 and SURC-2 experiments. The comparison of the calculations with measurements showed that the aerosol concentration was overpredicted by up to one order of magnitude. However, this discrepancy was partly resulted from that the comparison was made at the different locations. The releases of FP simulants were predicted by the code within one to several orders of magnitude. The largest difference was shown in the comparison of the Mo release. It was found through the present analysis that further improvements are needed for models on the chemistry and the vaporization of the molten core. In order to discuss more detail, the database of chemical species and related thermodynamic properties contained in CORCON-Mod3 should be extended.

Acknowledgment

One of authors (Jinquan Yan) would like to express sincere gratitude to Dr. Atsuo Kosaka, former director of Department of Reactor Safety Research of JAERI, for his hearty assistance on the assignment under Scientist Exchange Program by Science and Technology Agency of Japan. The authors are grateful to Mr. Norihiro Yamano and Mr. Akihide Hidaka of Severe Accident Research Laboratory of JAERI for their helpful comments on this report.

References

[1] USNRC, "Severe Accident Risks: an Assessment for Five U.S. Nuclear Power Plants", NUREG-1150, 1990.

[2] E. R. Copus, et al., "Core-Concrete Interactions Using Molten Steel with Zirconium on a Basaltic Basemat: The SURC-4 Experiment", NUREG/CR-4994 SAND87-2008, 1989.

[3] E. R. Copus, et al., "Core-Concrete Interactions Using Molten Urania with Zirconium on a Limestone Concrete Basemat: The SURC-1 Experiment", NUREG/CR-5443 SAND90-0087, 1992.

Large discrepancies were found between the calculations and the measurements for composition and amount of released gases. In the analysis of the experiment on the oxidic melt interaction with limestone concrete, CORCON-Mod3 largely overpredicted the total amount of released gas by a factor of up to 2 along with a quite different gas composition. Regarding the MCCI experiments with basaltic concrete, the calculations for the total amount of gas generated showed reasonable agreement with the experimental observation. However, the continuous release of reduced products (H_2 and CO) of concrete decomposed gases could not be reproduced by CORCON-Mod3. The difference between the experimental results and calculations might indicate that a kinetic approach is required for the chemical reactions between metallic materials and concrete decomposed gases.

The VANESA calculations were performed for the SURC-4 and SURC-2 experiments. The comparison of the calculations with measurements showed that the aerosol concentration was overpredicted by up to one order of magnitude. However, this discrepancy was partly resulted from that the comparison was made at the different locations. The releases of FP simulants were predicted by the code within one to several orders of magnitude. The largest difference was shown in the comparison of the Mo release. It was found through the present analysis that further improvements are needed for models on the chemistry and the vaporization of the molten core. In order to discuss more detail, the database of chemical species and related thermodynamic properties contained in CORCON-Mod3 should be extended.

Acknowledgment

One of authors (Jinquan Yan) would like to express sincere gratitude to Dr. Atsuo Kosaka, former director of Department of Reactor Safety Research of JAERI, for his hearty assistance on the assignment under Scientist Exchange Program by Science and Technology Agency of Japan. The authors are grateful to Mr. Norihiro Yamano and Mr. Akihide Hidaka of Severe Accident Research Laboratory of JAERI for their helpful comments on this report.

References

[1] USNRC, "Severe Accident Risks: an Assessment for Five U.S. Nuclear Power Plants", NUREG-1150, 1990.

[2] E. R. Copus, et al., "Core-Concrete Interactions Using Molten Steel with Zirconium on a Basaltic Basemat: The SURC-4 Experiment", NUREG/CR-4994 SAND87-2008, 1989.

[3] E. R. Copus, et al., "Core-Concrete Interactions Using Molten Urania with Zirconium on a Limestone Concrete Basemat: The SURC-1 Experiment", NUREG/CR-5443 SAND90-0087, 1992.

Large discrepancies were found between the calculations and the measurements for composition and amount of released gases. In the analysis of the experiment on the oxidic melt interaction with limestone concrete, CORCON-Mod3 largely overpredicted the total amount of released gas by a factor of up to 2 along with a quite different gas composition. Regarding the MCCI experiments with basaltic concrete, the calculations for the total amount of gas generated showed reasonable agreement with the experimental observation. However, the continuous release of reduced products (H_2 and CO) of concrete decomposed gases could not be reproduced by CORCON-Mod3. The difference between the experimental results and calculations might indicate that a kinetic approach is required for the chemical reactions between metallic materials and concrete decomposed gases.

The VANESA calculations were performed for the SURC-4 and SURC-2 experiments. The comparison of the calculations with measurements showed that the aerosol concentration was overpredicted by up to one order of magnitude. However, this discrepancy was partly resulted from that the comparison was made at the different locations. The releases of FP simulants were predicted by the code within one to several orders of magnitude. The largest difference was shown in the comparison of the Mo release. It was found through the present analysis that further improvements are needed for models on the chemistry and the vaporization of the molten core. In order to discuss more detail, the database of chemical species and related thermodynamic properties contained in CORCON-Mod3 should be extended.

Acknowledgment

One of authors (Jinquan Yan) would like to express sincere gratitude to Dr. Atsuo Kosaka, former director of Department of Reactor Safety Research of JAERI, for his hearty assistance on the assignment under Scientist Exchange Program by Science and Technology Agency of Japan. The authors are grateful to Mr. Norihiro Yamano and Mr. Akihide Hidaka of Severe Accident Research Laboratory of JAERI for their helpful comments on this report.

References

[1] USNRC, "Severe Accident Risks: an Assessment for Five U.S. Nuclear Power Plants", NUREG-1150, 1990.

[2] E. R. Copus, et al., "Core-Concrete Interactions Using Molten Steel with Zirconium on a Basaltic Basemat: The SURC-4 Experiment", NUREG/CR-4994 SAND87-2008, 1989.

[3] E. R. Copus, et al., "Core-Concrete Interactions Using Molten Urania with Zirconium on a Limestone Concrete Basemat: The SURC-1 Experiment", NUREG/CR-5443 SAND90-0087, 1992.

[4] E. R. Copus, et al., "Core-Concrete Interactions Using Molten UO_2 with Zirconium on a Basaltic Basemat: The SURC-2 Experiment", NUREG/CR-5564 SAND90-1022, 1992.

[5] E. R. Copus, et al., "Experimental Results of Core-Concrete Interactions Using Molten Steel with Zirconium", NUREG/CR-4794 SAND86-2638, 1990.

[6] H. Alsmeyer, et al., "BETA Experiments on Zirconium Oxidation and Aerosol Release during Melt-Concrete Interaction", Proceedings of the Second OECD CSNI Specialist Meeting on Core Debris Concrete Interactions, Karlsruhe, Germany, 1992.

[7] B. R. Sehgal, et al., "ACE program phase C: Fission Product Release From Molten Corium Concrete Interactions (MCCI)", Proceedings of the Second OECD CSNI Specialist Meeting on Core Debris Concrete Interactions, Karlsruhe, Germany, 1992.

[8] Y. Maruyama, et al., "Analysis of MCCI Tests in ALPHA and ACE Programs with CORCON-Mod3", Trans. 1994 Annual Mtg. of Atomic Energy Society of Japan, March, 1994 (in Japanese).

[9] R. K. Cole, et al., "CORCON-Mod2: A Computer Code Program for Analysis of Molten-Core Concrete Interactions", NUREG/CR-3920 SAND84-1246, 1984.

[10] D. R. Bradley, et al., "CORCON-Mod3: An Integrated Computer Model for Analysis of Molten Core-Concrete Interactions", NUREG/CR-5843, 1993.

[11] M. Reimann, et al., "The WECHSL-Mod2 Code: A Computer Program for the Interaction of a Core Melt with Concrete including the Long Term Behavior", KfK 4477, 1989.

[12] M. G. Plys, et al., "Modeling and Validation Progress with MAAP 4 DECOMP", Proceedings of the Second OECD CSNI Specialist Meeting on Core Debris Concrete Interactions, Karlsruhe, Germany, 1992.

[13] A. Hidaka, et al., "Analysis of ACE MCCI Test L6 with the CORCON/VANESA Code", Proc. the Second OECD(NEA)CSNI Specialist Meeting on Molten Core Debris-Concrete Interactions, Karlsruhe, Germany, 1-3 April 1992, KfK5108 NEA/CSNI/R(92)10, November, 1992.

[14] D. A. Powers, et al., "VANESA: A Mechanistic Model of Radionuclide Release and Aerosol Generation during Core Debris Interactions with Concrete", NUREG/CR-4308, 1986.

Table 1 Summary of major experimental conditions for SURC series

	Simulated Molten Core		Concrete Basemat		FP Simulants		Max. Power (kW)
	Composition	Mass (kg)	Type	Diameter (m)	Materials	Mass (kg)	
SURC-1	UO_2 (63 w/o) ZrO_2 (27 w/o) Zr (10 w/o)	200.8	Limestone	0.4	$BaMoO_4$ La_2O_3 CeO_2 Nb_2O_5	1.0 0.75 0.75 0.864	~90
SURC-2	UO_2 (69.1 w/o) ZrO_2 (22.6 w/o) Zr (8.3 w/o)	203.9	Basaltic	0.4	$BaMoO_4$ La_2O_3 CeO_2 Nb_2O_5	1.0 0.75 0.75 0.864	~85
SURC-3	Stainless Steel Zr	50 5	Limestone	0.216	Te Mo BaO ZrO_2 CeO_2 La_2O_3 Nb_2O_5	0.5 0.5 0.5 0.5 0.5 0.5 0.5	~35
SURC-4	Stainless Steel Zr	200 20	Basaltic	0.4	Mo Te La_2O_3 CeO_2 Nb_2O_5	2.0 0.5 1.17 1.23 1.1	~60

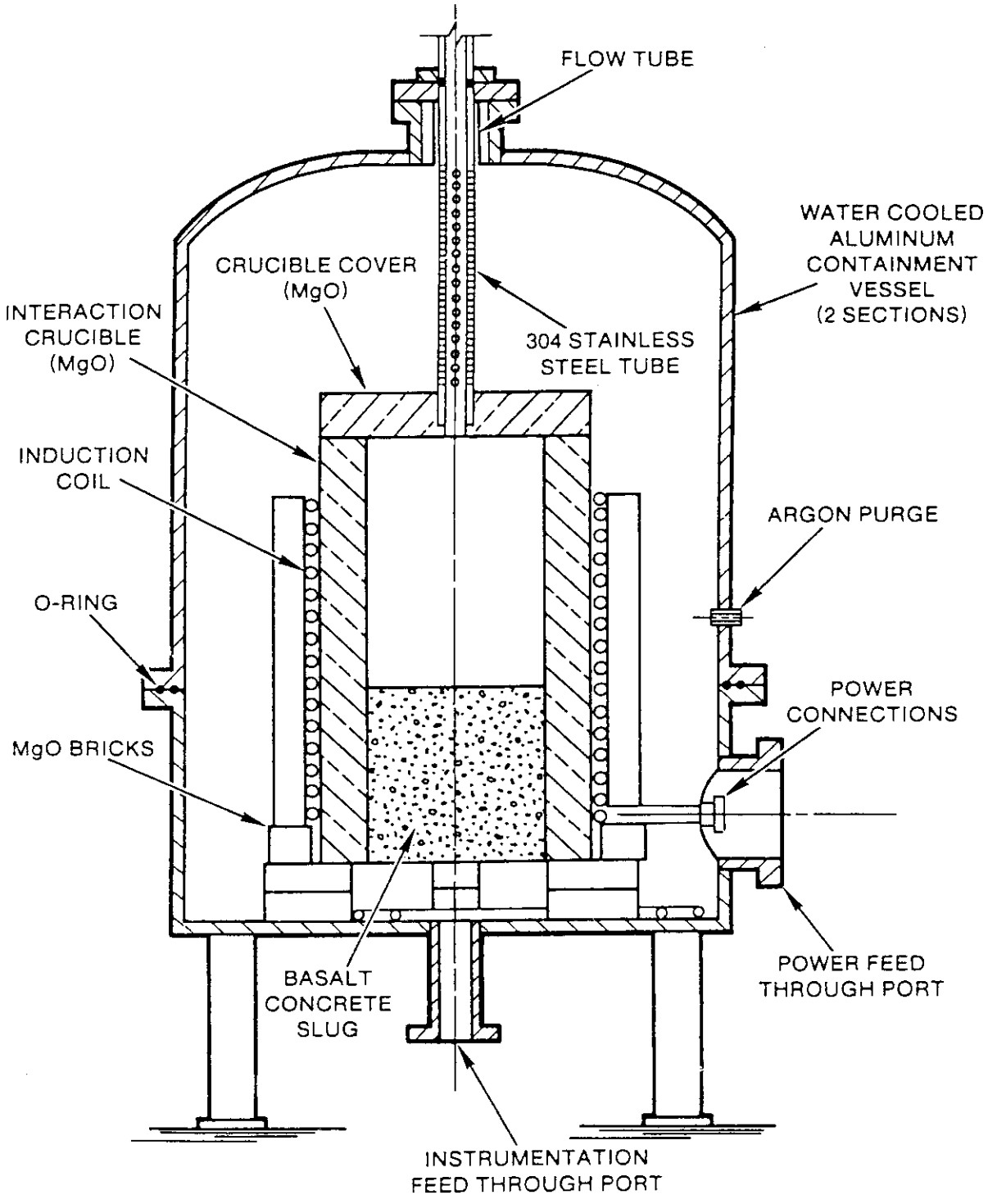

Fig. 1 Schematic diagram of SURC experimental apparatus

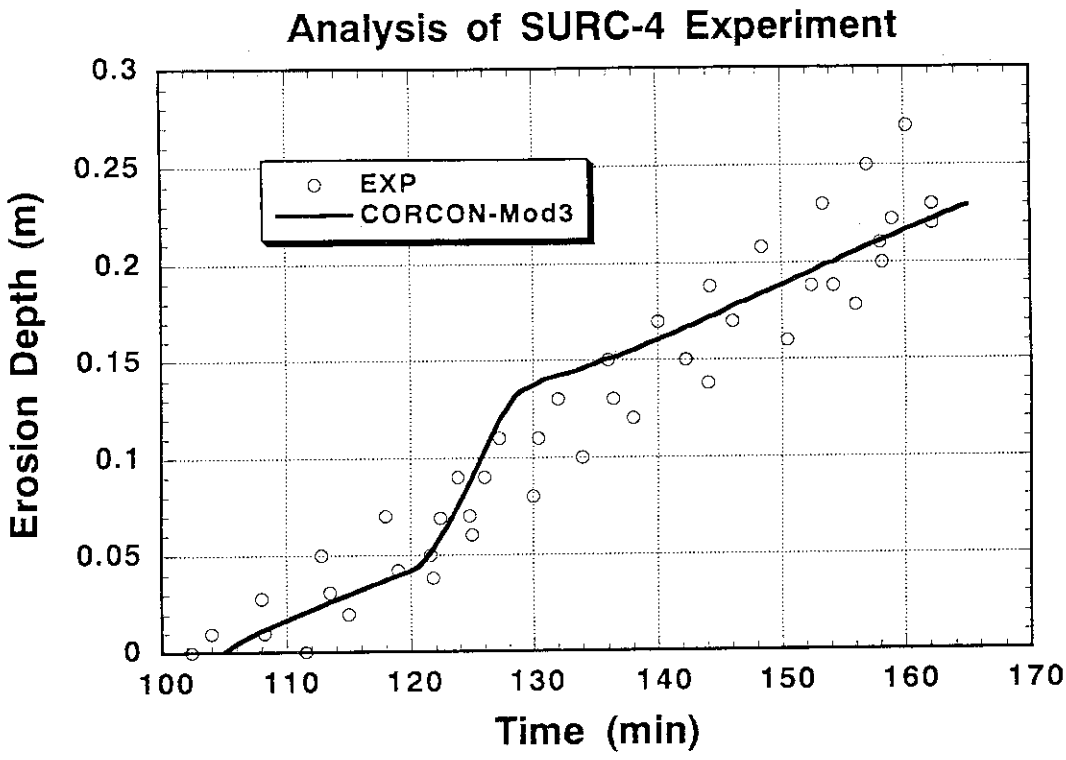

Fig. 2 a Comparison of concrete erosion depth for SURC-4 experiment (two laryers assumption)

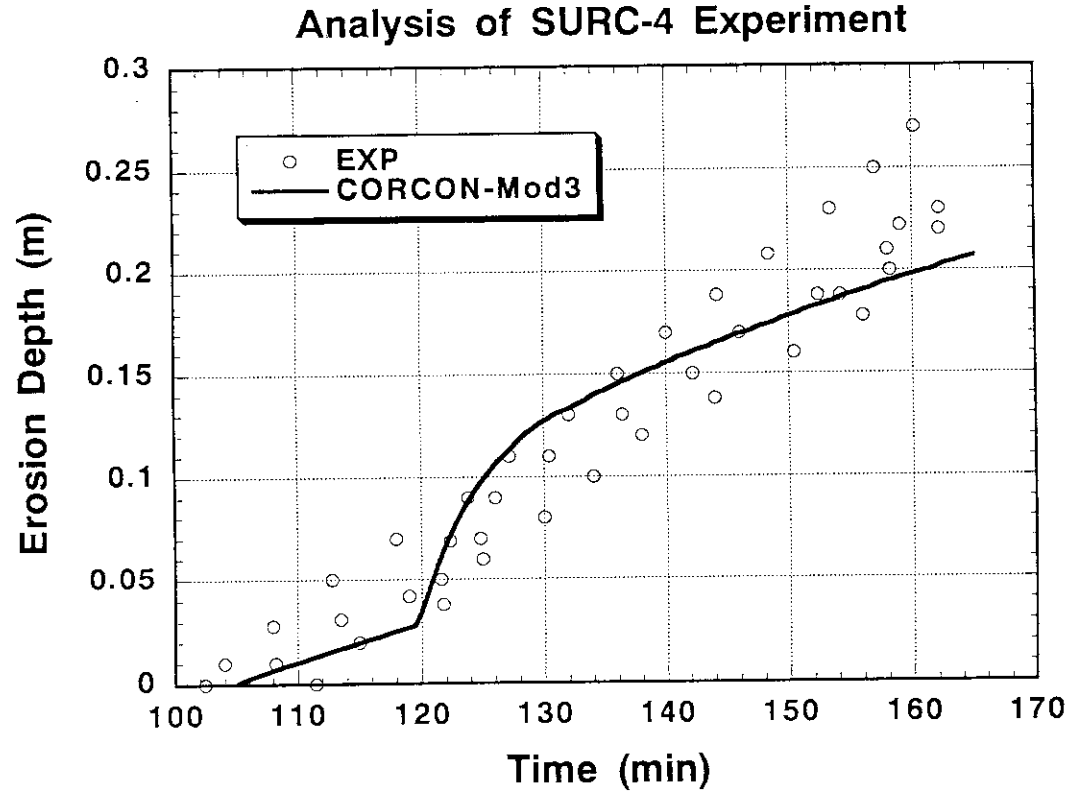

Fig. 2 b Comparison of concrete erosion depth for SURC-4 experiment (mixing layer assumption)

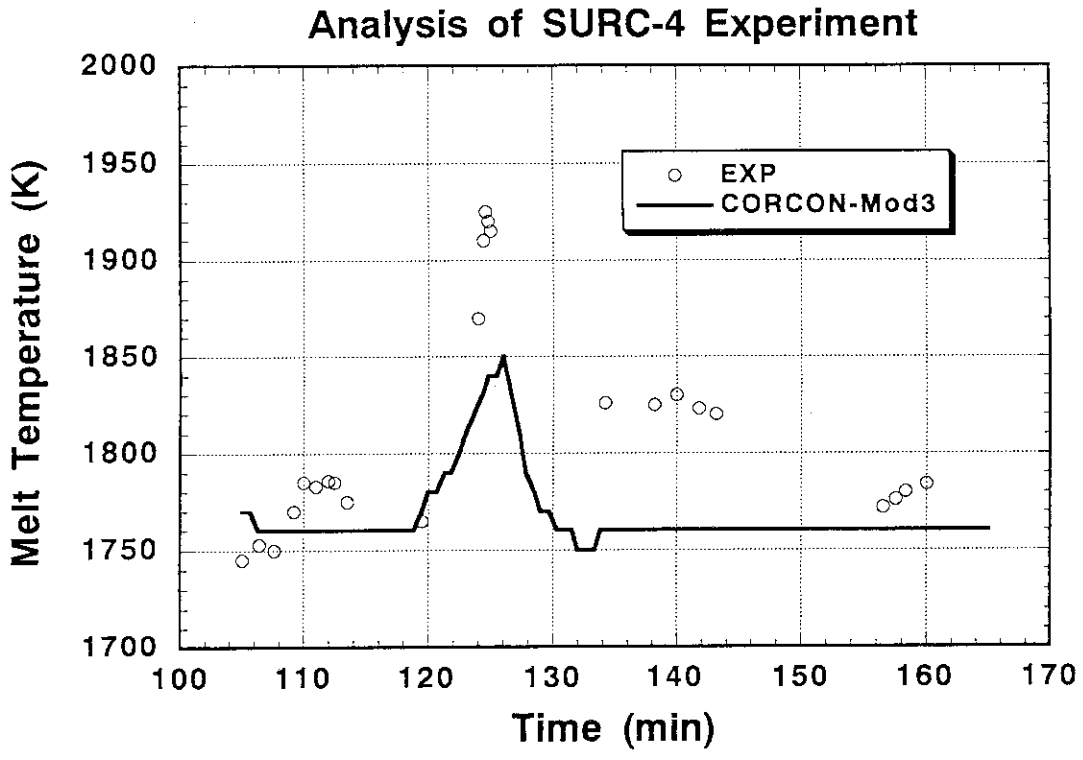

Fig. 3 a Comparison of melt temperature history for SURC-4 experiment (two layers assumption)

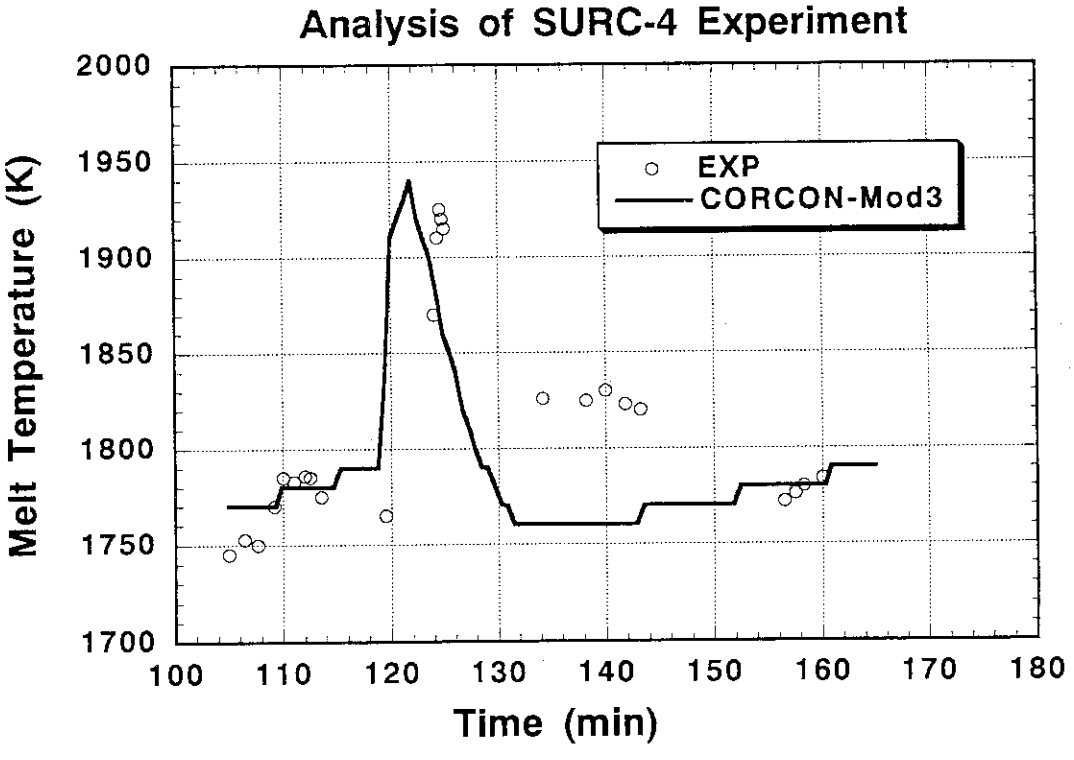

Fig. 3 b Comparison of melt temperature history for SURC-4 experiment (mixing layer assumption)

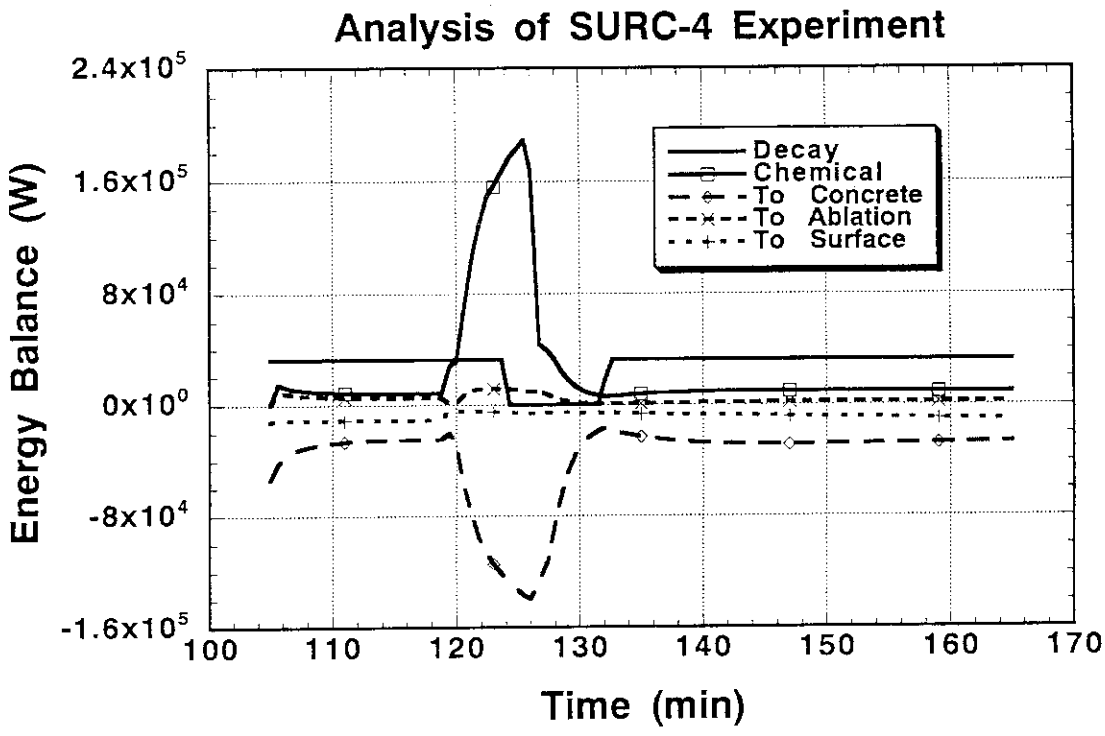

Fig. 4 a Energy balance calculation for SURC-4 experiment (two layers assumption)

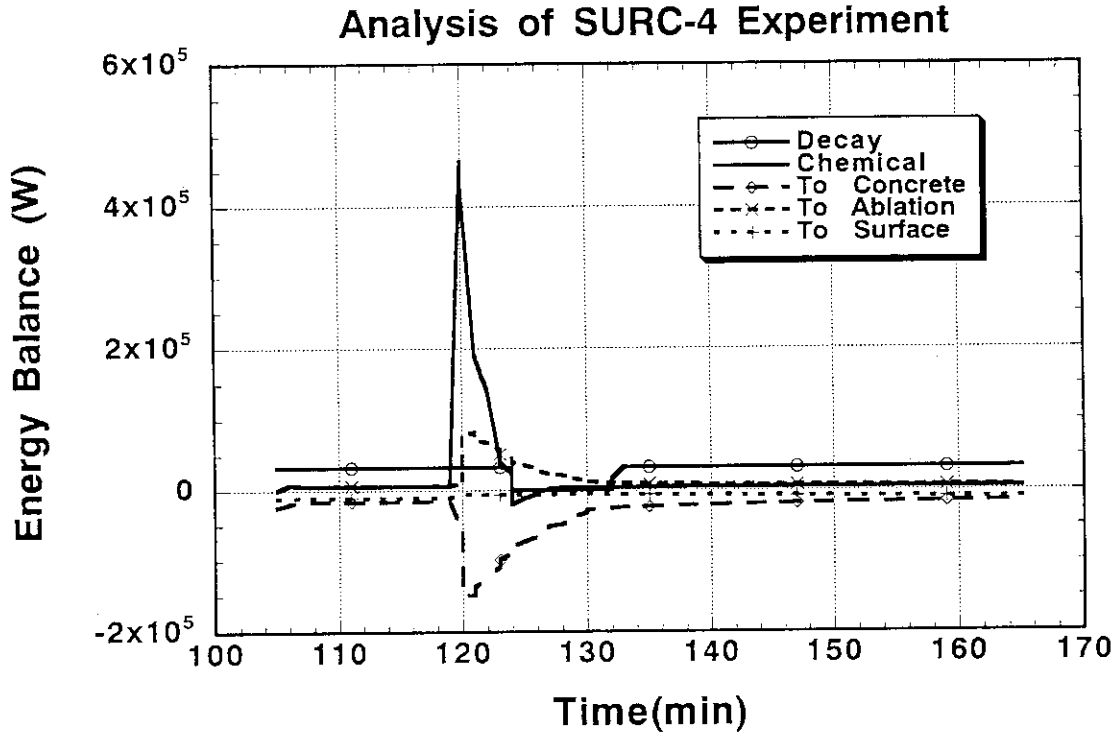

Fig. 4 b Energy balance calculation for SURC-4 experiment (mixing layer assumption)

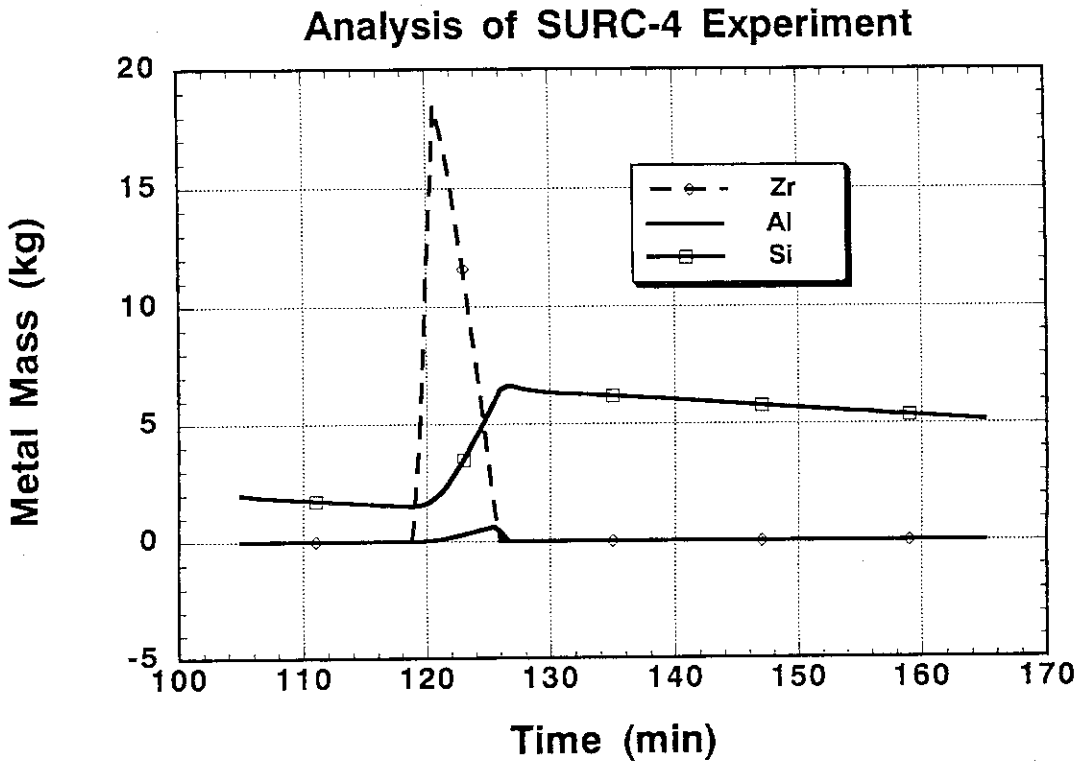

Fig. 5 a Metal mass in melt calculated for SURC-4 experiment (two layers assumption)

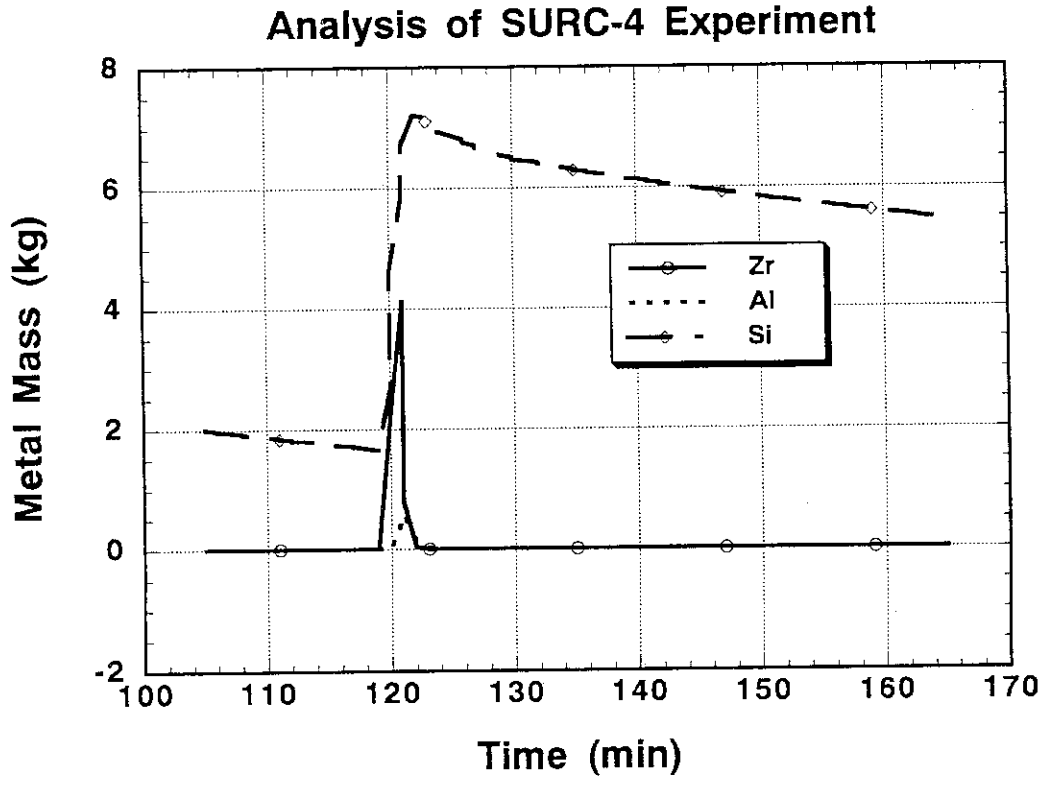

Fig. 5 b Metal mass in melt calculated for SURC-4 experiment (mixing layer assumption)

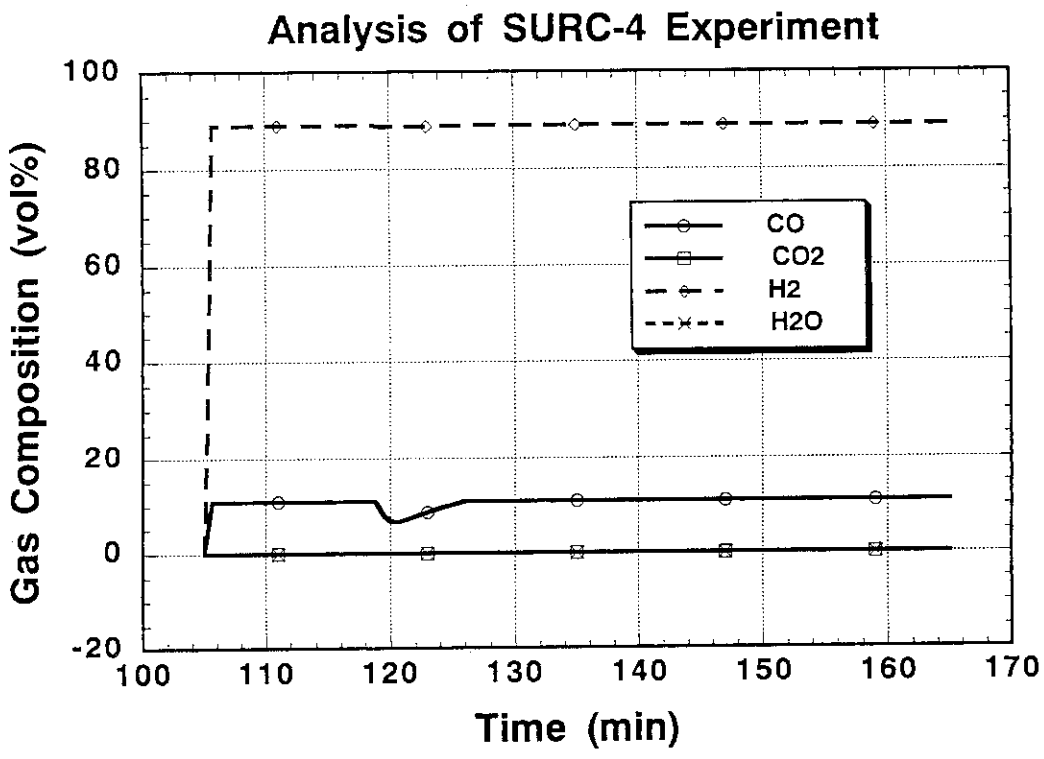

Fig. 6 Prediction of released gas composition for SURC-4 experiment

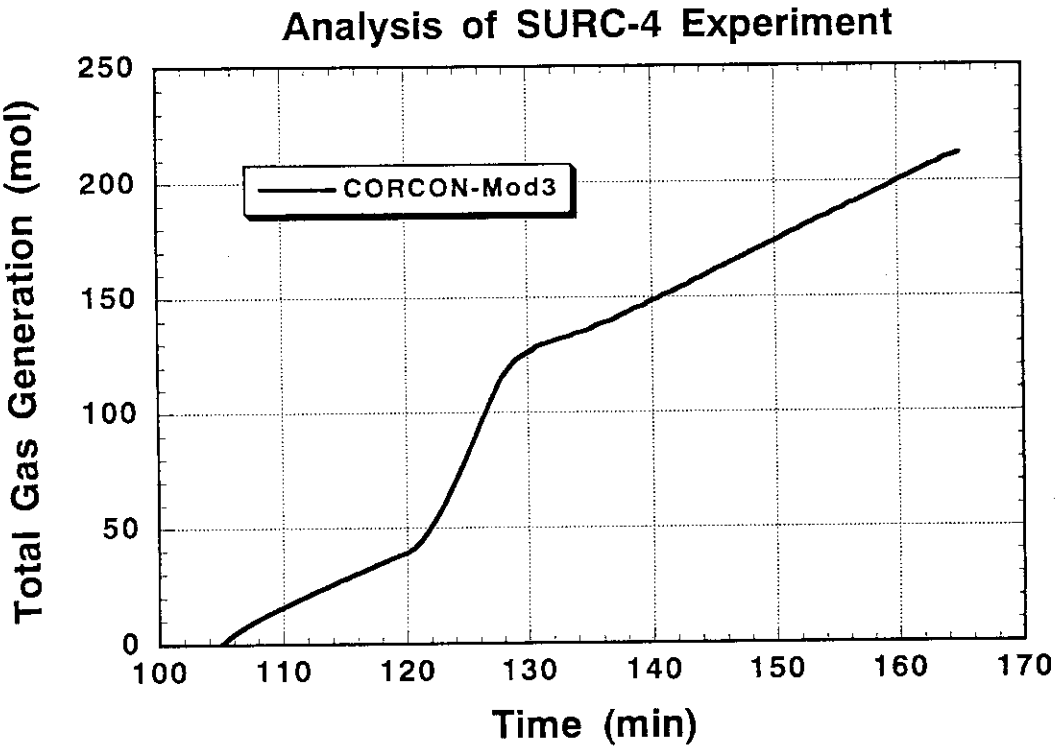

Fig. 7 Prediction of total gas generation for SURC-4 experiment

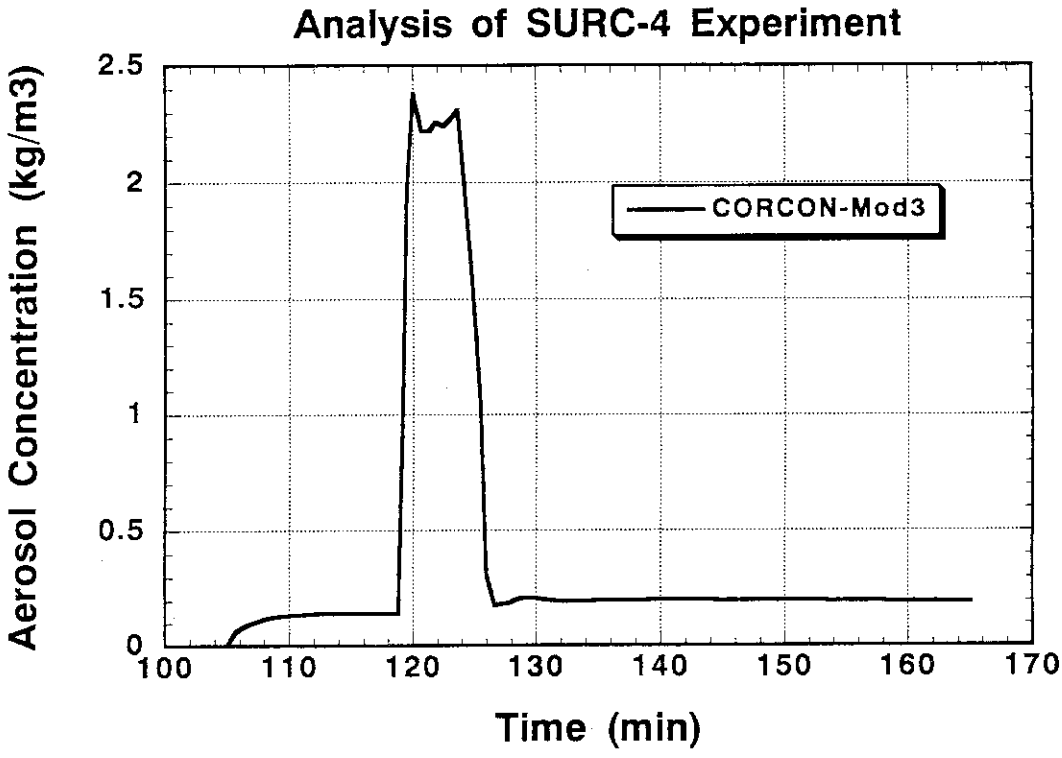

Fig. 8 Calculated aerosol concentration for SURC-4 experiment

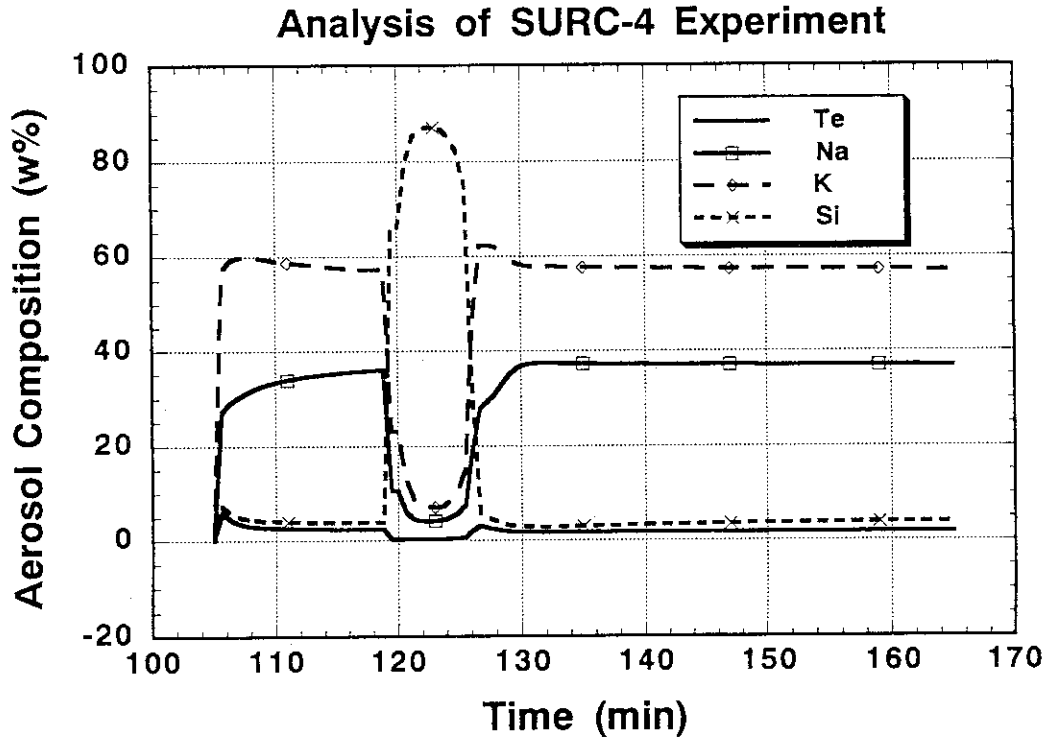

Fig. 9 Calculated aerosol composition for SURC-4 experiment (1)

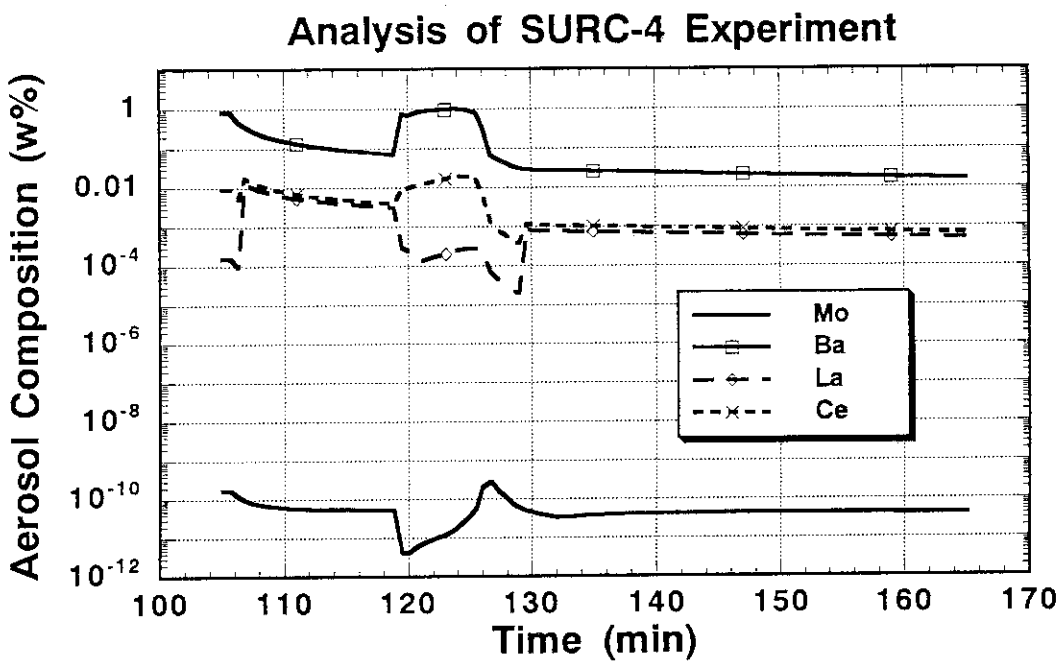

Fig. 10 Calculated aerosol composition for SURC-4 experiment (2)

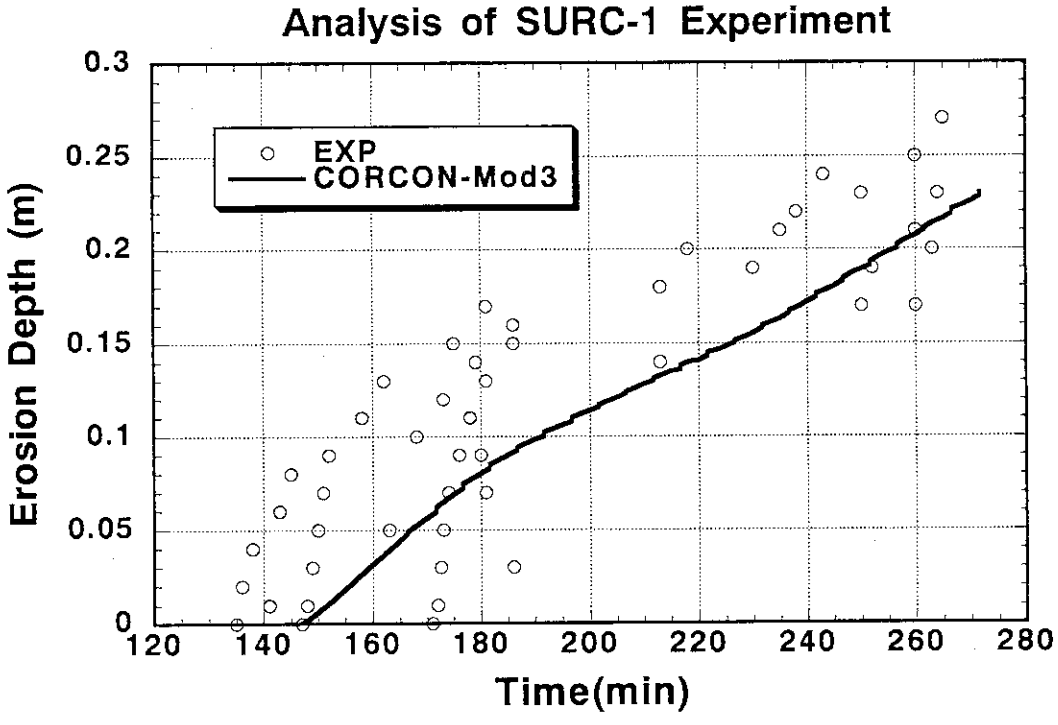

Fig. 11 Comparison of concrete erosion depth for SURC-1 experiment

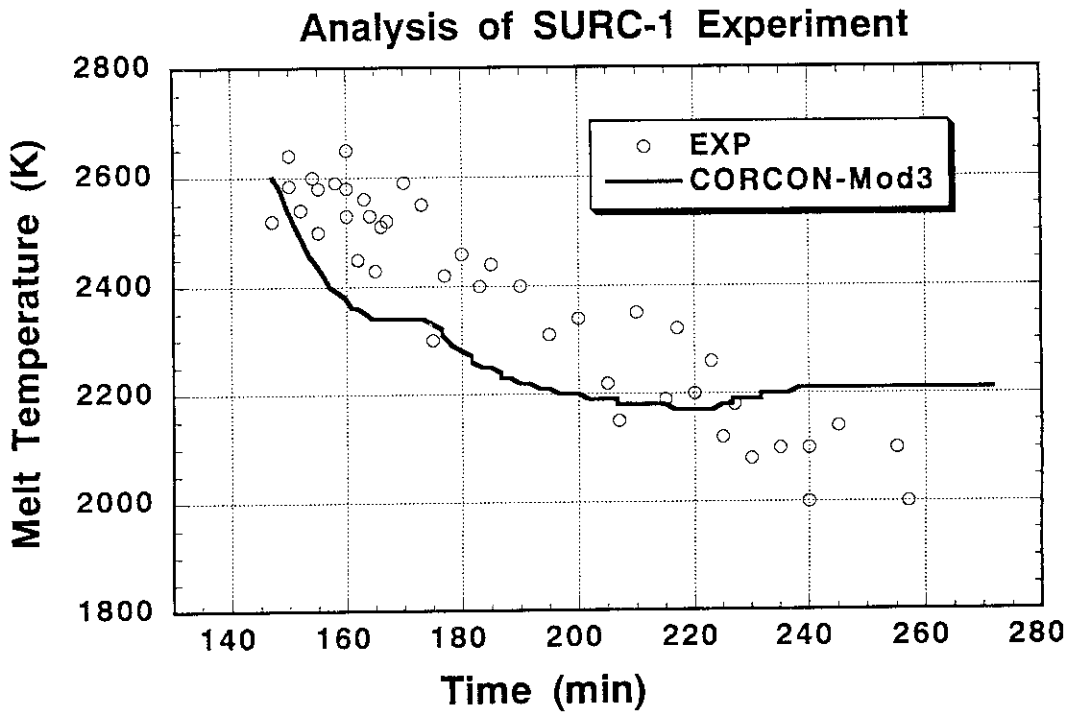

Fig. 12 Comparison of melt temperature history for SURC-1 experiment

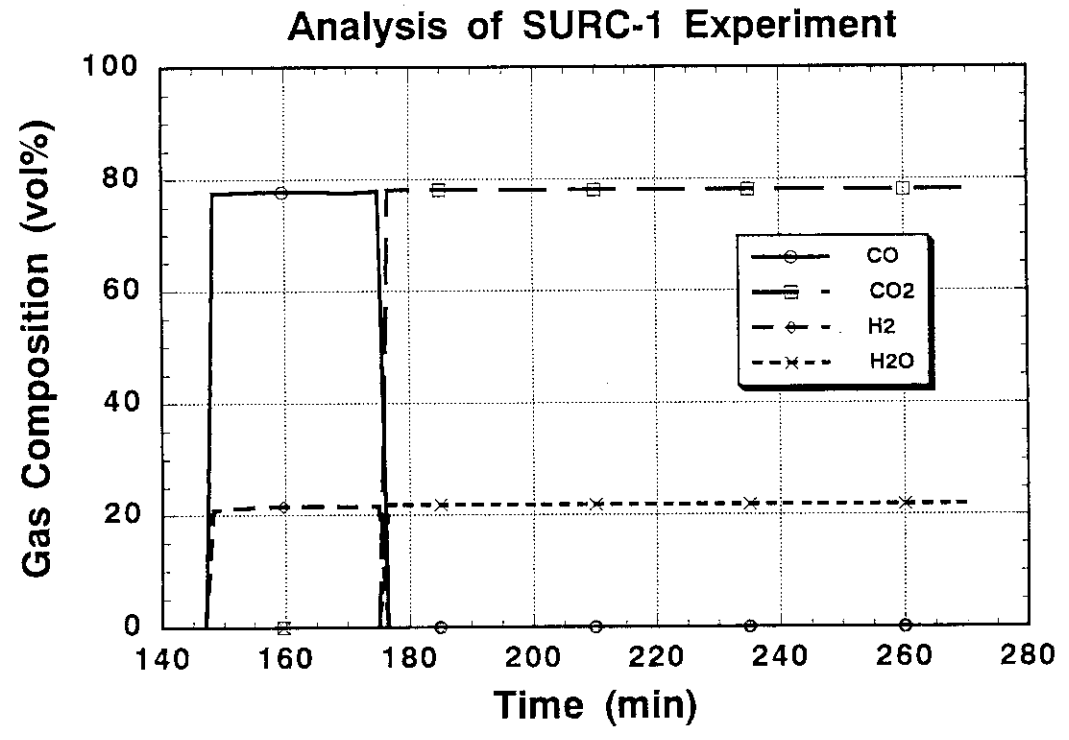

Fig. 13 Prediction of released gas composition for SURC-1 experiment

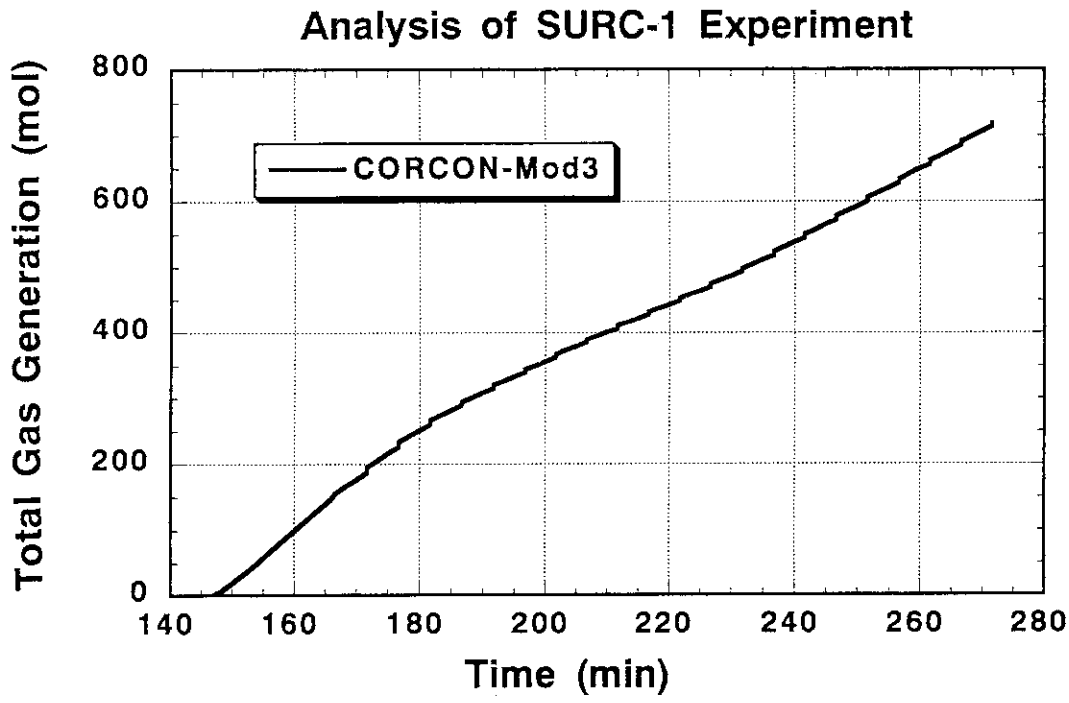

Fig. 14 Prediction of total gas generation for SURC-1 experiment

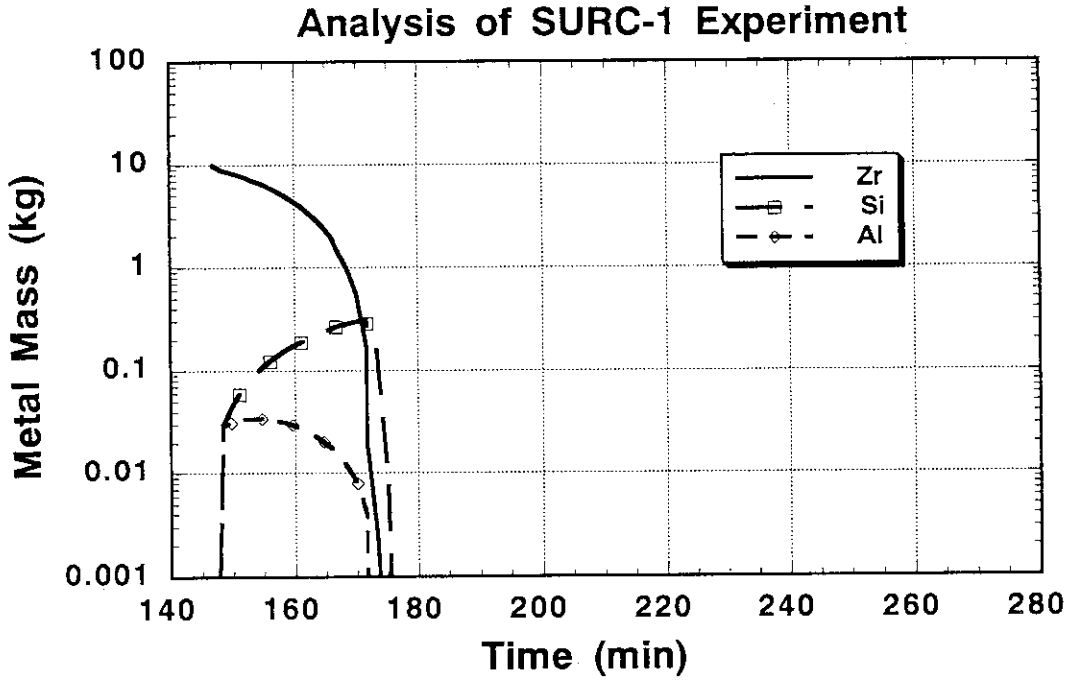

Fig. 15 Metal mass in melt calculated for SURC-1 experiment

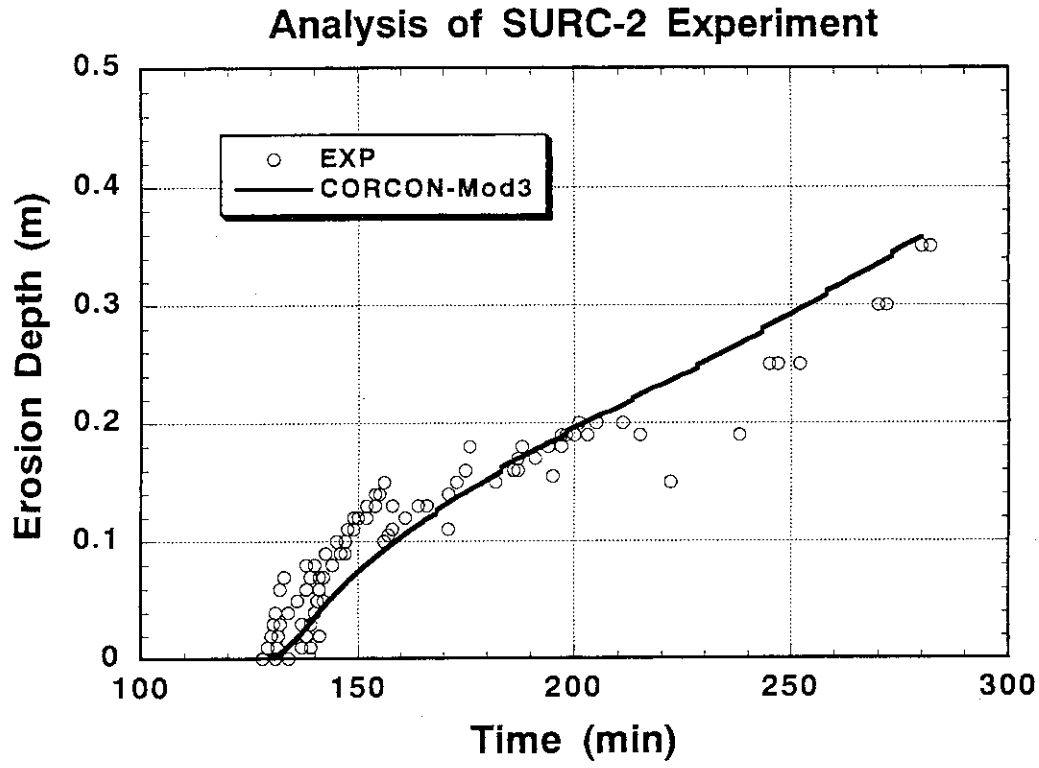

Fig. 16 Comparison of concrete erosion depth for SURC-2 experiment

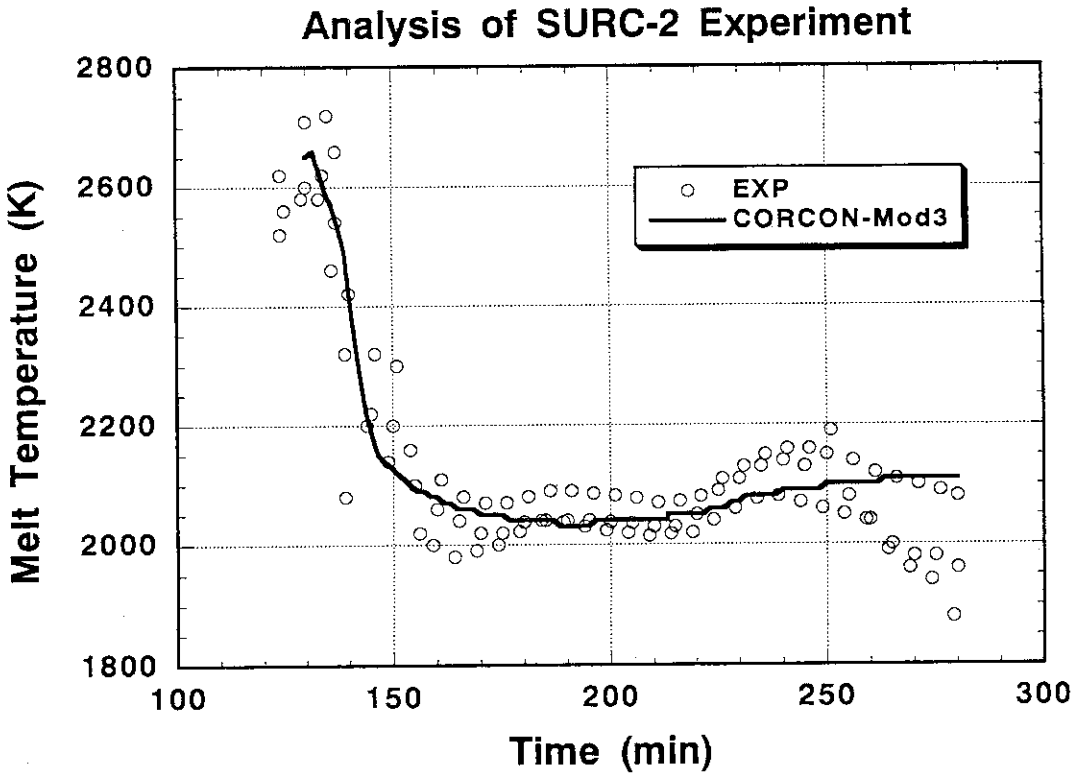

Fig. 17 Comparison of melt temperature history for SURC-2 experiment

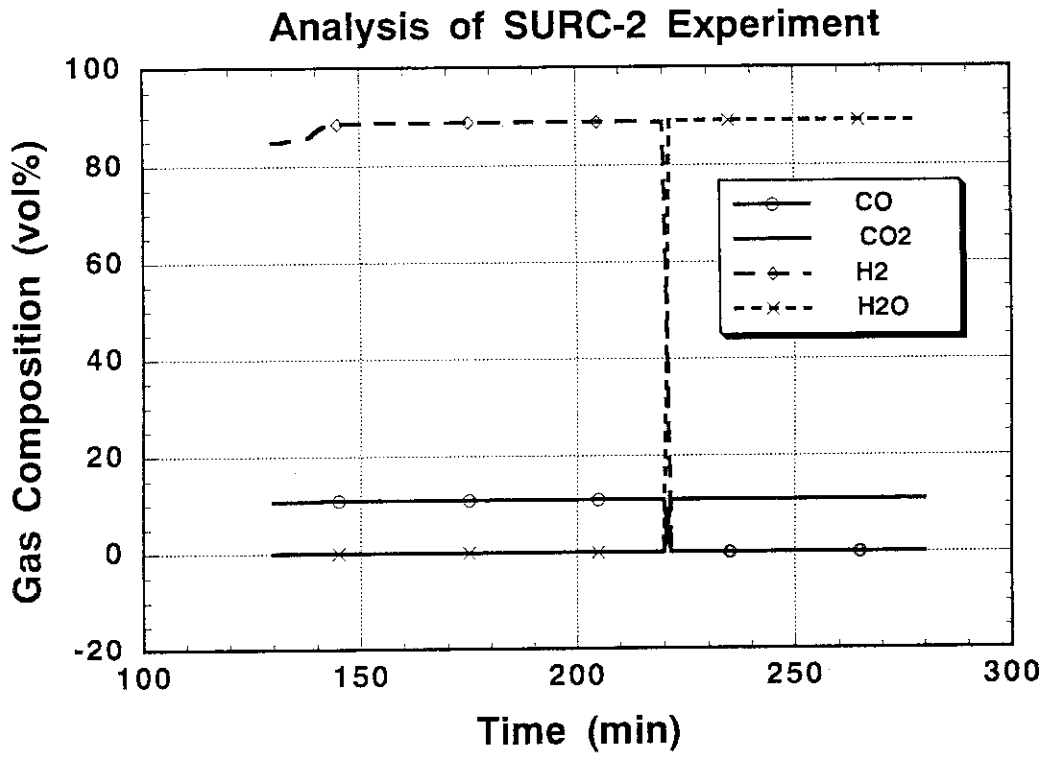

Fig. 18 Prediction of released gas composition for SURC-2 experiment

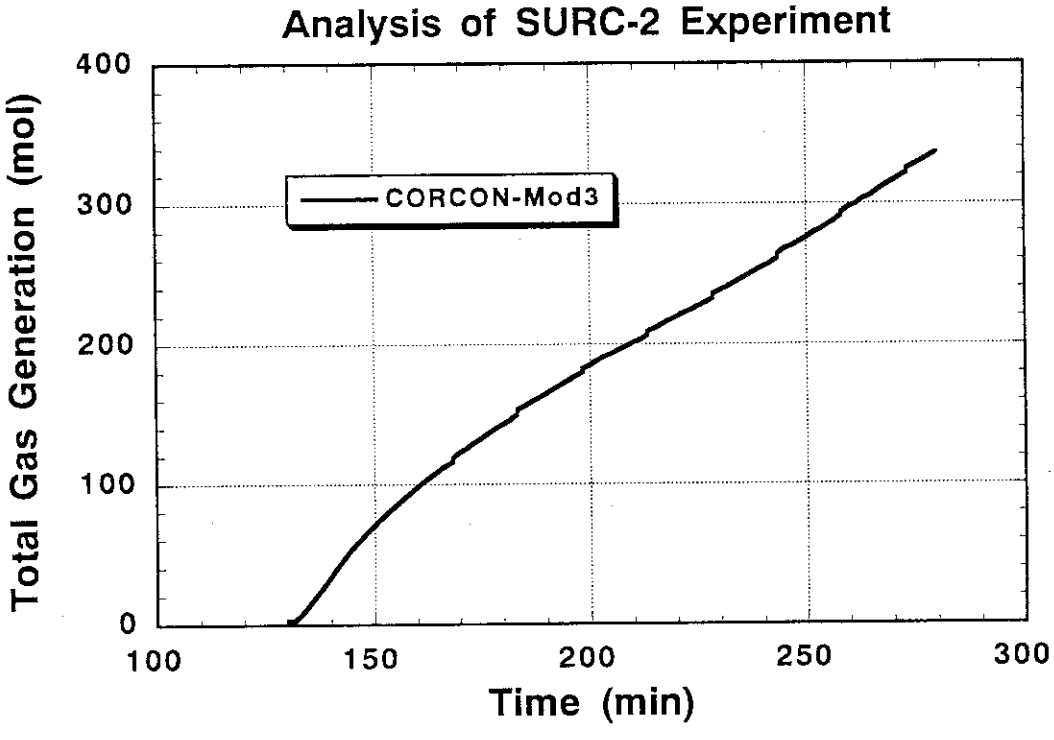

Fig. 19 Prediction of total gas generation for SURC-2 experiment

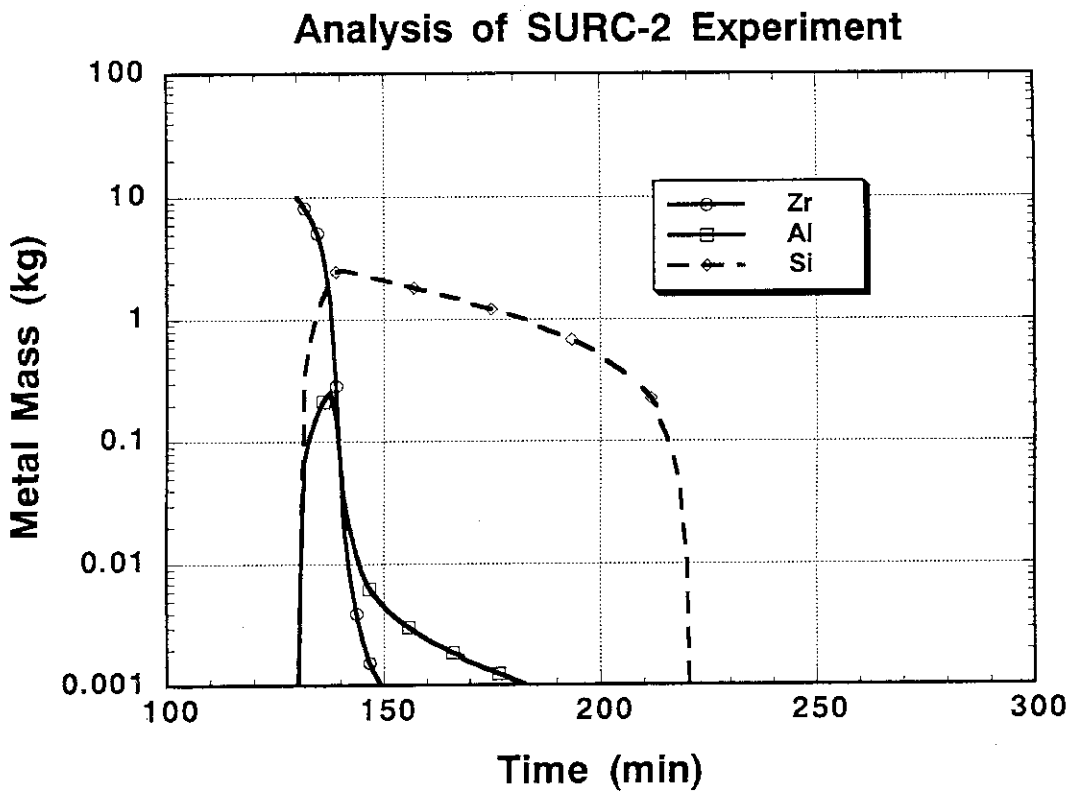

Fig. 20 Metal mass in melt calculated for SURC-2 experiment

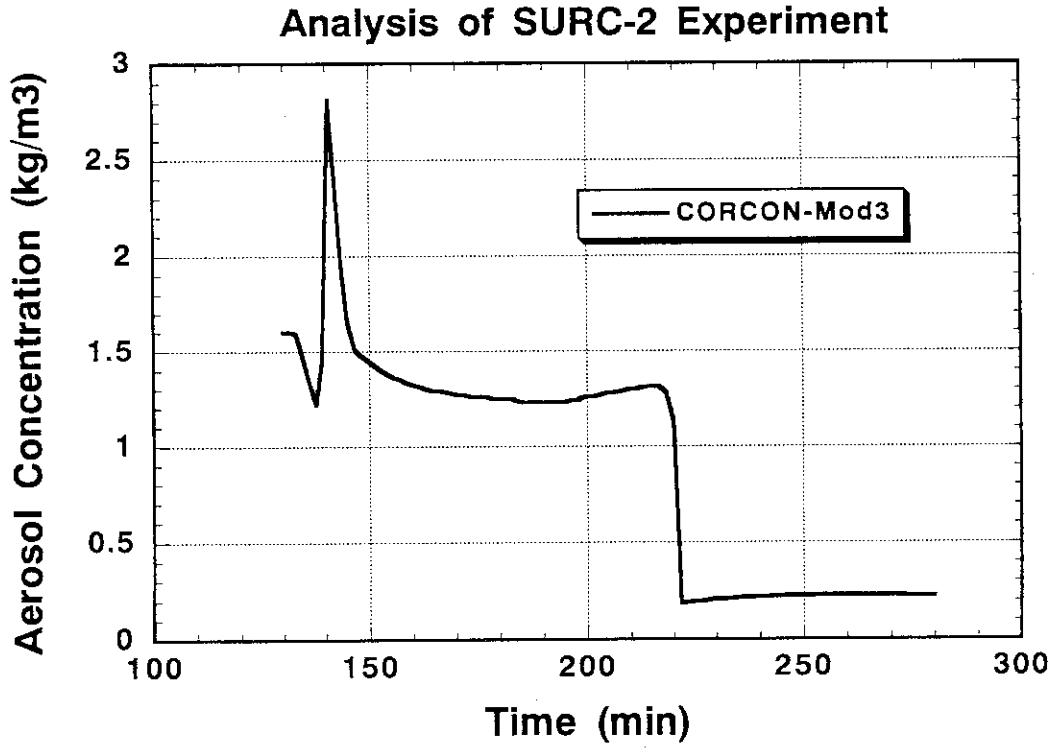

Fig. 21 Calculated aerosol concentration for SURC-2 experiment

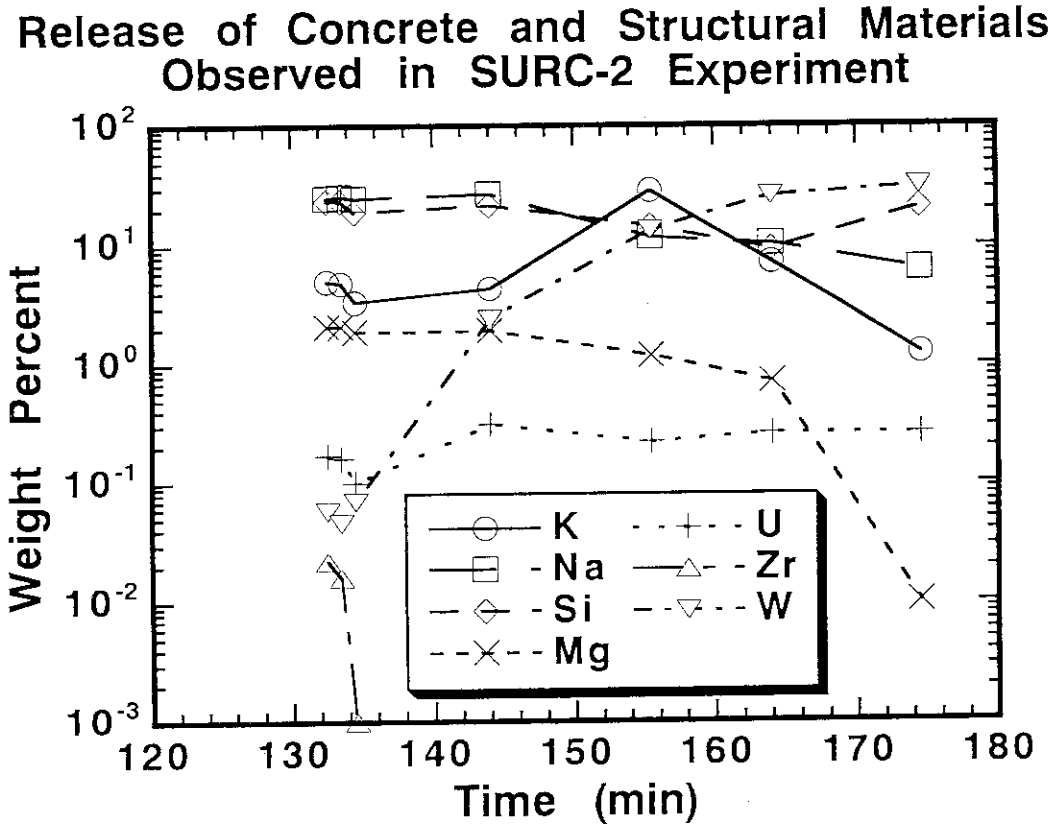

Fig. 22 Measured composition of released concrete and structural materials in SURC-2 experiment

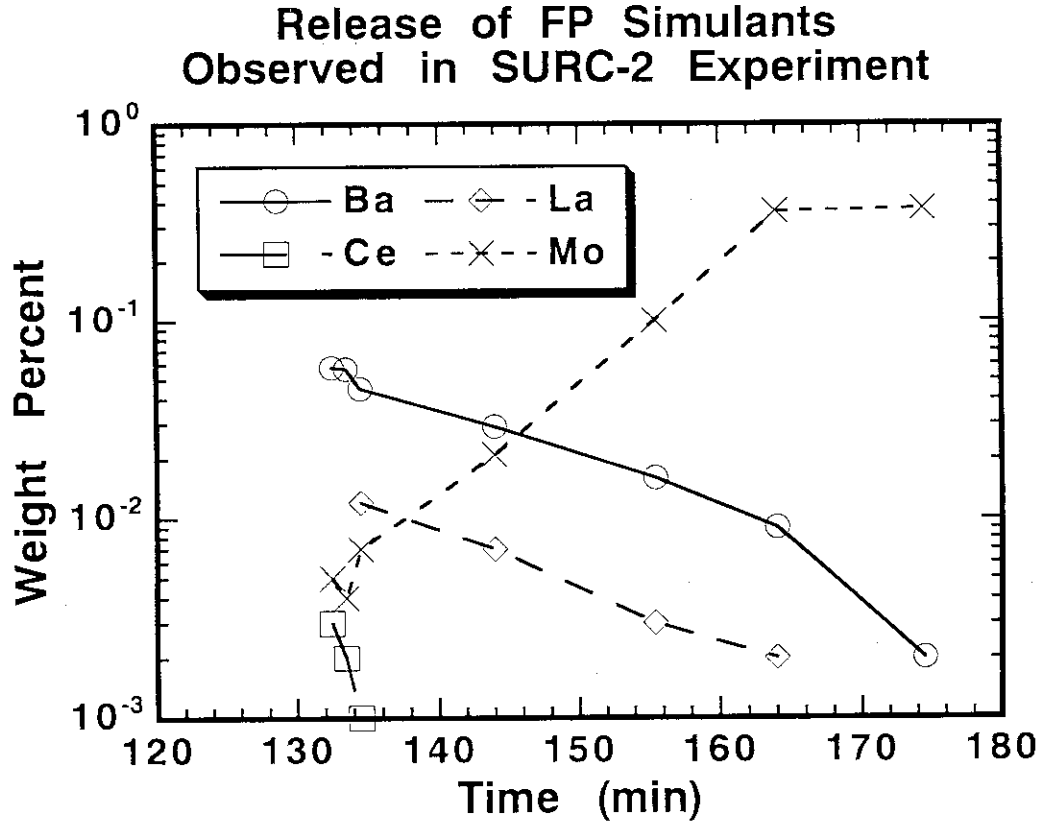

Fig. 23 Measured composition of released FP simulants in SURC-2 experiment

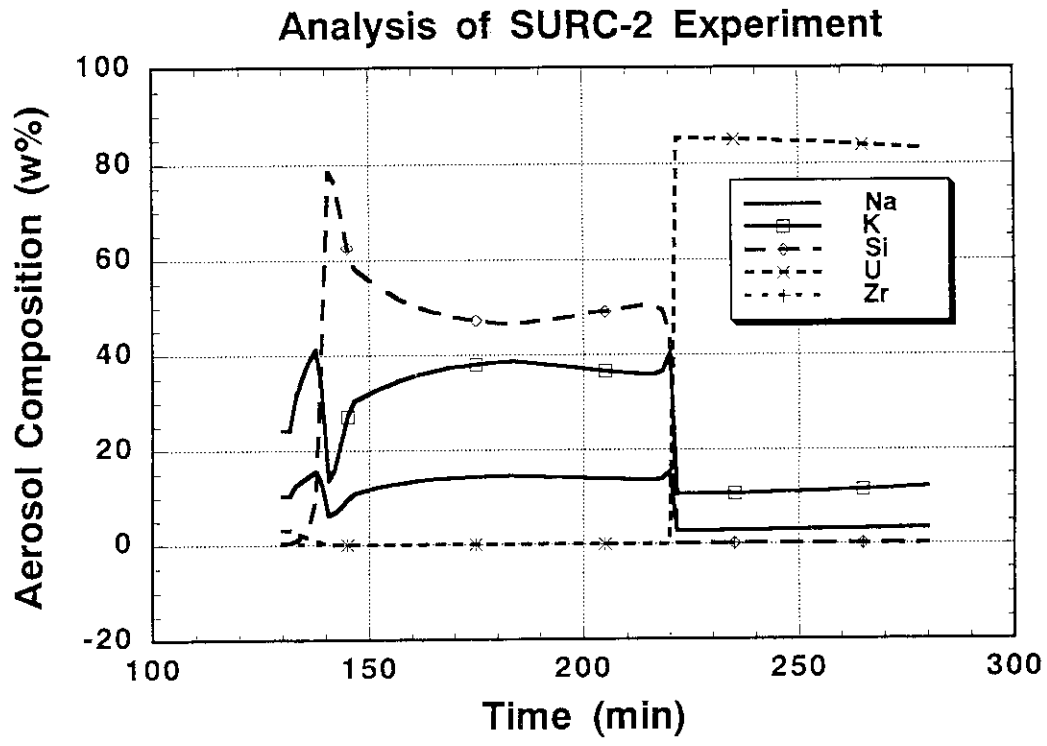

Fig. 24 Calculated aerosol composition for SURC-2 experiment (melt and concrete materials)

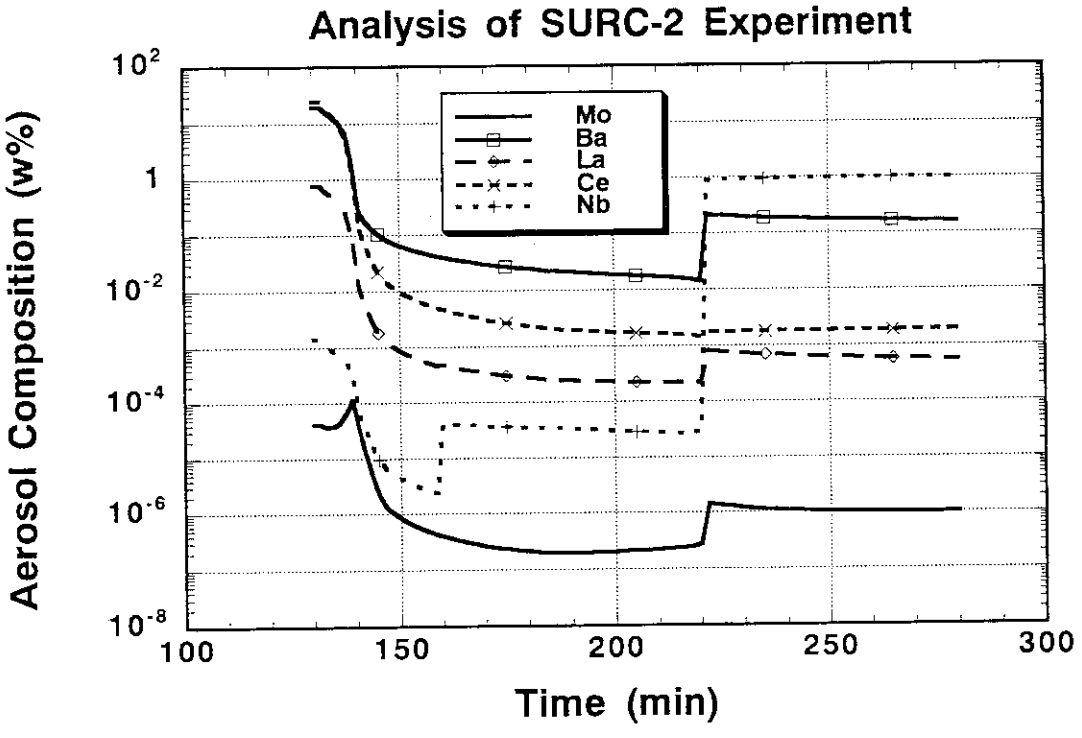

Fig. 25 Calculated aerosol composition for SURC-2 experiment (fission product simulants)